

Gain of Toxicity from ALS/FTD-Linked Repeat Expansions in C9ORF72 Is Alleviated by Antisense Oligonucleotides Targeting GGGGCC-Containing RNAs

Highlights

- C9ORF72 repeat expansions cause age-, repeat-size-, and expression-dependent toxicity
- Acquired toxicity, not loss of function, is a major contributor to C9orf72 disease
- Absence of C9ORF72 in mice produces splenomegaly and enlarged cervical lymph nodes
- ASO-induced decreases in repeat RNA mitigate C9ORF72-associated phenotypes *in vivo*

Authors

Jie Jiang, Qiang Zhu,
Tania F. Gendron, ..., Frank Rigo,
Don W. Cleveland,
Clotilde Lagier-Tourenne

Correspondence

dclleveland@ucsd.edu (D.W.C.),
clagier-tourenne@mgh.harvard.edu
(C.L.-T.)

In Brief

Hexanucleotide expansions in C9ORF72 are the most frequent genetic cause of ALS and FTD. Jiang et al. establish gain of toxicity from repeat-containing RNA, and not loss of C9ORF72 function, as a central disease mechanism and establish the feasibility of ASO-mediated therapy.



Gain of Toxicity from ALS/FTD-Linked Repeat Expansions in C9ORF72 Is Alleviated by Antisense Oligonucleotides Targeting GGGGCC-Containing RNAs

Jie Jiang,^{1,3,17} Qiang Zhu,^{1,17} Tania F. Gendron,^{4,17} Shahram Saberi,³ Melissa McAlonis-Downes,¹ Amanda Seelman,¹ Jennifer E. Stauffer,³ Paymaan Jafar-nejad,⁵ Kevin Drenner,¹ Derek Schulte,³ Seung Chun,⁵ Shuying Sun,¹ Shuo-Chien Ling,^{1,6} Brian Myers,¹ Jeffery Engelhardt,⁵ Melanie Katz,⁵ Michael Baughn,^{1,2,3} Oleksandr Platoshyn,^{7,8} Martin Marsala,^{7,8,9} Andy Watt,⁵ Charles J. Heyser,³ M. Colin Ard,³ Louis De Muynck,^{10,11} Lillian M. Daugherty,⁴ Deborah A. Swing,¹² Lino Tessarollo,¹² Chris J. Jung,¹³ Arnaud Delpoux,^{2,14} Daniel T. Utzschneider,^{2,14} Stephen M. Hedrick,^{2,14} Pieter J. de Jong,¹³ Dieter Edbauer,¹⁵ Philip Van Damme,^{10,11} Leonard Petrucelli,⁴ Christopher E. Shaw,¹⁶ C. Frank Bennett,⁵ Sandrine Da Cruz,¹ John Ravits,³ Frank Rigo,⁵ Don W. Cleveland,^{1,2,3,*} and Clotilde Lagier-Tourenne^{1,3,18,*}

¹Ludwig Institute for Cancer Research

²Department of Cellular and Molecular Medicine

³Department of Neurosciences

University of California, San Diego, La Jolla, CA 92093, USA

⁴Department of Neuroscience, Mayo Clinic, 4500 San Pablo Road, Jacksonville, FL 32224, USA

⁵Ionis Pharmaceuticals, 2855 Gazelle Court, Carlsbad, CA 92010, USA

⁶Department of Physiology, National University of Singapore, 12 Science Drive 2, Singapore 117549, Singapore

⁷Department of Anesthesiology, University of California, San Diego, La Jolla, CA 92093, USA

⁸Neuroregeneration Laboratory, Sanford Consortium for Regenerative Medicine, 2880 Torrey Pines Scenic Drive, La Jolla, CA 92037, USA

⁹Institute of Neurobiology, Slovak Academy of Sciences, Soltesovej 9, 04001 Kosice, Slovakia

¹⁰Laboratory of Neurobiology, Vesalius Research Center, Experimental Neurology, Department of Neurosciences, KU Leuven/VIB, 3000 Leuven, Belgium

¹¹Department of Neurology, University Hospitals Leuven, 3000 Leuven, Belgium

¹²Mouse Cancer Genetics Program, National Cancer Institute, Frederick, MD 21702, USA

¹³Children's Hospital Oakland Research Institute, 5700 Martin Luther King Jr Way, Oakland, CA 94609, USA

¹⁴Molecular Biology Section, Division of Biological Sciences, University of California, San Diego, La Jolla, CA 92093, USA

¹⁵German Center for Neurodegenerative Diseases (DZNE), Ludwig-Maximilians University and Munich Cluster of Systems Neurology (SyNergy), Feodor-Lynen Strasse 17, 81377 Munich, Germany

¹⁶Institute of Psychiatry, King's College London, London WC2R 2LS, UK

¹⁷Co-first author

¹⁸Present address: MassGeneral Institute for Neurodegenerative Disease, Department of Neurology, Massachusetts General Hospital, Harvard Medical School, Charlestown, MA 02129, USA

*Correspondence: dcleveland@ucsd.edu (D.W.C.), clagier-tourenne@mgh.harvard.edu (C.L.-T.)

<http://dx.doi.org/10.1016/j.neuron.2016.04.006>

SUMMARY

Hexanucleotide expansions in C9ORF72 are the most frequent genetic cause of amyotrophic lateral sclerosis and frontotemporal dementia. Disease mechanisms were evaluated in mice expressing C9ORF72 RNAs with up to 450 GGGGCC repeats or with one or both C9orf72 alleles inactivated. Chronic 50% reduction of C9ORF72 did not provoke disease, while its absence produced splenomegaly, enlarged lymph nodes, and mild social interaction deficits, but not motor dysfunction. Hexanucleotide expansions caused age-, repeat-length-, and expression-level-dependent accumulation of RNA foci and dipeptide-repeat proteins synthesized by AUG-independent translation, accompanied by loss of hippocampal neurons, increased anxiety, and impaired cognitive function. Single-dose injection of antisense

oligonucleotides (ASOs) that target repeat-containing RNAs but preserve levels of mRNAs encoding C9ORF72 produced sustained reductions in RNA foci and dipeptide-repeat proteins, and ameliorated behavioral deficits. These efforts identify gain of toxicity as a central disease mechanism caused by repeat-expanded C9ORF72 and establish the feasibility of ASO-mediated therapy.

INTRODUCTION

Amyotrophic lateral sclerosis (ALS) and frontotemporal dementia (FTD) are two devastating adult-onset neurodegenerative diseases with distinct clinical features but common pathological features and genetic causes (Ling et al., 2013). Hexanucleotide GGGGCC repeat expansions in a noncoding region of the C9ORF72 gene are the most common inherited cause of ALS and FTD (DeJesus-Hernandez et al., 2011; Renton et al., 2011).

Proposed mechanisms by which *C9ORF72* repeat expansions cause disease (referred to as C9ALS/FTD) include loss of *C9ORF72* protein function and gain of toxicity (Gendron et al., 2014; Ling et al., 2013).

A reduction in *C9ORF72* function (i.e., haploinsufficiency) is supported by decreased expression of *C9ORF72* mRNAs in patient tissues resulting from DNA and histone hypermethylation with partial silencing of the repeat-containing allele (Belzil et al., 2013; DeJesus-Hernandez et al., 2011; Gijssenick et al., 2012; Liu et al., 2014; Xi et al., 2013, 2015). RNA gain of toxicity has been proposed to arise from folding of repeat-containing RNAs into stable structures that sequester RNA-binding proteins to nuclear RNA foci, a mechanism originally established for myotonic dystrophy (reviewed by Wojciechowska and Krzyzosiak, 2011). Indeed, foci containing sense GGGGCC or antisense GGCCCC repeat RNA are present in tissues from C9ALS/FTD patients (DeJesus-Hernandez et al., 2011; Gendron et al., 2013; Lagier-Tourenne et al., 2013; Mizielska et al., 2013; Mori et al., 2013a; Zu et al., 2013). Several RNA-binding proteins appear enriched in sense RNA foci (Cooper-Knock et al., 2014; Donnelly et al., 2013; Lee et al., 2013; Mori et al., 2013b; Sareen et al., 2013; Xu et al., 2013), but evidence supporting a loss of function of these proteins is lacking.

Another proposed disease mechanism from *C9ORF72* repeat expansions is the production of aberrant dipeptide-repeat (DPR) proteins through repeat-associated non-AUG-dependent (RAN) translation, a phenomenon discovered in spinocerebellar ataxia type 8 and myotonic dystrophy (Zu et al., 2011). In C9ALS/FTD patients, five DPR proteins—poly(GA), poly(GR), poly(GP), poly(PA), and poly(PR)—are produced from all reading frames of either sense or antisense repeat-containing RNAs (Ash et al., 2013; Gendron et al., 2013; Mori et al., 2013a, 2013c; Zu et al., 2013). DPR proteins form p62-positive, TDP-43-negative inclusions, with poly(GA), poly(GP), and poly(GR) aggregates being the most abundant (Mackenzie et al., 2014; Mori et al., 2013c). Poly(GP) and poly(GA) can also be detected by immunassay in patient-derived cultured cells, postmortem tissues, and cerebrospinal fluid (Gendron et al., 2015; Su et al., 2014; van Blitterswijk et al., 2015). Overexpressing (Mizielska et al., 2014; Wen et al., 2014; Yang et al., 2015) or exogenously exposing (Kwon et al., 2014) cells and other model systems to high levels of arginine-containing DPR proteins induces rapid cell death. Other studies have reported poly(GA) to be particularly prone to aggregation and to confer toxicity (Gendron et al., 2015; May et al., 2014; Schludi et al., 2015; Zhang et al., 2014, 2016). Lastly, a recent flurry of studies found that nucleocytoplasmic transport is impaired in C9ALS/FTD (Boeynaems et al., 2016; Freibaum et al., 2015; Jovićić et al., 2015; Zhang et al., 2015, 2016), although the exact roles of RNA foci and/or DPR proteins in this pathway are not yet resolved. Indeed, divergent outcomes were reported regarding the toxicity of repeat-containing RNAs or DPR proteins in cell culture (Devlin et al., 2015; Kwon et al., 2014; Lee et al., 2013; May et al., 2014; Rossi et al., 2015; Schludi et al., 2015; Wen et al., 2014; Zhang et al., 2014; Zu et al., 2013), flies (Freibaum et al., 2015; Mizielska et al., 2014; Tran et al., 2015; Xu et al., 2013; Zhang et al., 2015), yeast (Jovićić et al., 2015), and mice (Chew et al., 2015; Hukema et al., 2014; O'Rourke et al., 2015; Peters et al., 2015; Zhang et al., 2016).

By production and analysis of mice in which one or both *C9orf72* alleles were inactivated, and multiple transgenic mouse lines expressing up to 450 *C9ORF72* hexanucleotide repeats, we tested disease mechanism(s) associated with C9ALS/FTD. Herein we show a repeat-length-dependent gain of toxicity, while chronic reduction of *C9ORF72* does not produce nervous system disease. Single-dose injection of antisense oligonucleotides (ASOs) that selectively target repeat-containing RNAs causes a rapid reduction in RNA foci and DPR proteins, while maintaining overall levels of *C9ORF72*-encoding mRNAs and producing a sustained alleviation of behavioral deficits.

RESULTS

Reduction in *C9ORF72* Is Well-Tolerated, but Splenomegaly and Enlarged Lymph Nodes Develop in Its Absence

To determine the consequence of loss of *C9ORF72* function in vivo, mice were generated in which a LacZ reporter replaced exons 2–6 of the endogenous *C9orf72* gene (Figure 1A). As expected, total *C9orf72* RNAs and the full-length 54 kD *C9ORF72* protein were reduced to 50% in brains of heterozygous *C9orf72*^{+/−} mice and were completely absent in homozygous *C9orf72*^{−/−} mice (Figures 1B and 1C). A β-galactosidase activity assay, used to assess endogenous *C9orf72* gene expression throughout the CNS, revealed broad expression of *C9orf72* not only in neurons of the gray matter as previously reported (Suzuki et al., 2013), but also in glial cells of white matter in various CNS regions, including the cerebellum and spinal cord (Figures S1A and S1B, available online). Further evidence confirming substantial expression of the *C9orf72* gene in glial cells was obtained using high-throughput sequencing of translated RNAs purified from BacTRAP transgenic mice that express EGFP-tagged ribosomal protein L10a in defined cell populations (Heiman et al., 2008). *C9orf72* RNAs were identified in all three cell types tested, with relative abundances of 2.5:1:1 in motor neurons, astrocytes, and oligodendrocytes, respectively (Figure S1C). No overt neuropathology developed in *C9orf72*^{+/−} or *C9orf72*^{−/−} mice, and no increase in GFAP-positive astrocytes or IBA-1-positive microglia occurred in brain and spinal cord (Figures S1D and S1E).

The reduction in *C9ORF72* to 50% of its normal level, as reported in C9ALS/FTD patients, was well tolerated with *C9orf72*^{+/−} mice surviving into adulthood with a normal body weight and no signs of disease (Figures 1D–1F). In contrast, although *C9orf72*^{−/−} mice were born in the expected Mendelian ratio with no change in survival through 11 months of age, only 7% of mice survived to 20 months of age (Figure 1D). *C9orf72* null mice showed reduced body weight (Figure 1E), splenomegaly (Figure 1F), and enlarged cervical lymph nodes (Figure S1F) by 12 months of age. The spleen size was comparable in *C9orf72*^{+/−} mice (80.33 ± 0.88 mg, $n = 3$, mean \pm SEM) versus wild-type littermates (80 ± 0.41 mg, $n = 4$) at 18 months of age. Staining of CD3-positive T lymphocytes and CD45R/B220-positive B lymphocytes revealed disrupted architectures of the spleen and cervical lymph nodes in *C9orf72*^{−/−} mice (Figures S1G and S1H). Despite the enlarged size, the total number of lymphoid cells was not changed in the spleen, while the number

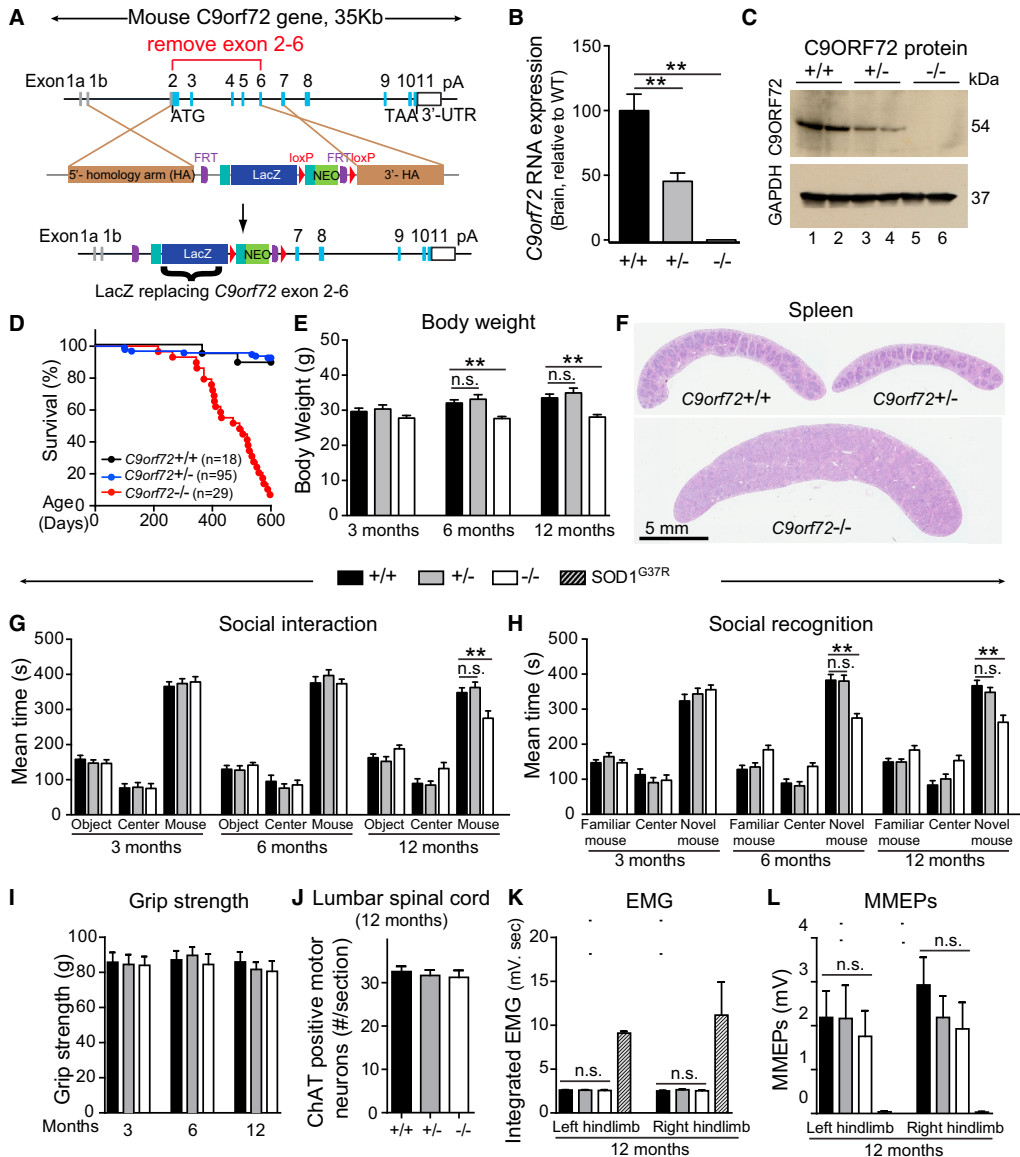


Figure 1. Reduction of C9ORF72 Is Well-Tolerated, but Complete Loss of C9ORF72 Induces Premature Death and Splenomegaly

(A) Targeting strategy to generate C9orf72 null mice with exons 2–6 replaced with β-galactosidase and neomycin (Neo) genes. Schematic shows (upper panel) the genomic region, (middle panel) targeting construct, and (lower panel) final targeted C9orf72 gene. Filled boxes correspond to exons. Open box represents the 3' untranslated region (3'-UTR).

(B) qRT-PCR measurement of mouse C9orf72 RNAs in brains of C9orf72^{+/+}, C9orf72^{+/-}, and C9orf72^{-/-} mice (n = 6 per group).

(C) Immunoblot demonstrating the levels of the 54 kD mouse C9ORF72 protein. GAPDH was used as a loading control.

(D) Survival curve up to 600 days.

(E) Body weights at 3, 6, and 12 months of age (n = 25 per genotype).

(F) Spleen sizes at 12 months of age.

(G–I) Behavioral performance measured at 3, 6, and 12 months of age (n = 25 animals per group). (G) Social interactions measured by the mean time spent with an object, in the center, or with a mouse. (H) Social recognition measured by the mean time spent with a familiar mouse, in the center, or with a novel mouse. (I) Hindlimb grip strength.

(J) Average number of ChAT-positive neurons per section in the anterior horn of lumbar spinal cord in 12-month-old mice (n = 4–5 per group).

(K and L) Resting electromyographic (EMG) recordings (K) and myogenic motor-evoked potentials (MMEPs) (L) in 12-month-old C9orf72 mice (n = 5 per genotype) or in end-stage transgenic mice expressing mutant SOD1^{G37R} (crosshatched bars, n = 2). Error bars represent SEM in biological replicates; n.s., not significant; *p < 0.05, **p < 0.01 using one-way ANOVA.

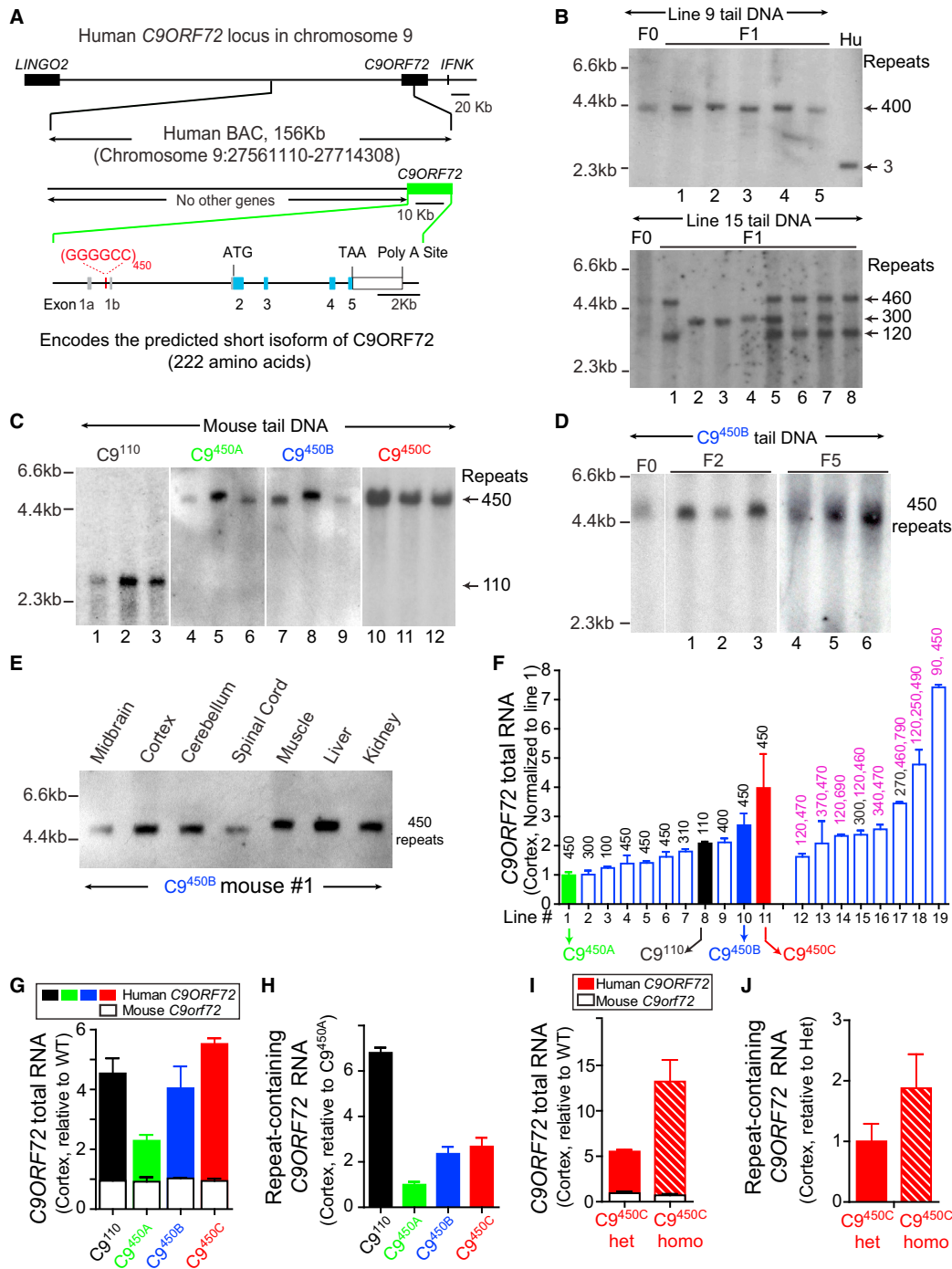


Figure 2. Generation of Multiple BAC Transgenic Mouse Lines Expressing Different Levels of a Human C9ORF72 Transgene with 100–700 GGGGCC Repeats

(A) Schematic of the human BAC containing 450 GGGGCC repeats in the first intron of a truncated human C9ORF72 gene. The coordinates of the BAC sequence on the University of California, Santa Cruz Genome Browser (Hg19) are indicated. No other gene is on the BAC.

(legend continued on next page)

of myeloid cells increased dramatically. Both lymphoid and myeloid cells were increased by more than an order of magnitude in the cervical lymph nodes (Figure S2A). In addition, *C9orf72* null mice showed decreased hemoglobin and packed cell volume, decreased percentage of lymphocytes, and increased percentage of neutrophils in blood (Figure S2B).

To determine whether partial or complete loss of *C9ORF72* triggered age-dependent cognitive and/or motor deficits, longitudinal assessment of strength, motor coordination, anxiety, sociability, and learning functions in cohorts of *C9orf72*^{+/+}, *C9orf72*^{-/-}, and *C9orf72*^{-/-} mice was performed. No behavioral abnormalities were observed in *C9orf72*^{-/-} mice at any of the ages tested (3, 6, and 12 months) (Figures 1G–H and S2C–S2H). By 12 months of age, *C9orf72* null mice developed mild social interaction (Figure 1G) and social recognition (Figure 1H) abnormalities compared with wild-type or heterozygous littermates. In addition, 12-month-old *C9orf72*^{-/-} mice developed mild motor deficits on a rotarod assay (Figure S2C) without differences in grip strength, gait, or general activity (Figures 1I, S2D, and S2E), or loss of ChAT-positive lower motor neurons (Figure 1J). Resting electromyographic (EMG) recordings were also normal in the gastrocnemius muscles of mice lacking *C9ORF72*, consistent with intact neuromuscular connectivity (Figure 1K). The amplitudes of myogenic motor-evoked potentials (MMEPs), a measure of connectivity of the entire neuromuscular unit, are comparable among *C9orf72*^{+/+}, *C9orf72*^{-/-}, and *C9orf72*^{-/-} mice (Figure 1L), in contrast to their almost complete loss in end-stage SOD1^{G37R} mice. Overall, *C9ORF72* reduction alone is not sufficient to cause C9ALS/FTD-associated phenotypes in mice.

BAC *C9ORF72* Transgenic Mouse Lines with Different Repeat Sizes and Expression Levels

To test a potential gain of toxicity from repeat expansions, transgenic mice were generated that express a bacterial artificial chromosome (BAC) with the human expanded *C9ORF72* gene from a C9ALS patient. The BAC includes 140 kb of sequence 5' to the *C9ORF72* exon 1a (including what is likely to be the complete promoter region) and exons 1–5 of the gene. The BAC does not encode the 54 kD *C9ORF72* protein (Figure 2A) (DeJesus-Hernandez et al., 2011). The interferon kappa gene, which lies within 23 kb 3' of *C9ORF72* on human chromosome 9, is not present, nor is any other known gene besides *C9ORF72*.

Thirty-two founder mice were generated in a C57BL6/C3H hybrid background and backcrossed to C57BL/6 mice. Founders from eight lines had either multiple repeat sizes that separated in subsequent generations (Figure 2B) or multiple

transgene copies with different repeat lengths at the same locus that segregated together (Figure S3A). Eleven lines contained a single repeat size that was stably inherited from filial (F0) to F5 generations in the large majority of mice (Figures 2B–D), albeit analysis of 42 littermates from one line identified three repeat contraction events (Figure S3B). At most, modest expansion was found within the CNS or peripheral tissues (Figures 2E, S3C, and S3D), in contrast to humans, for whom somatic heterogeneity and repeat instability have been reported, especially within the CNS (van Blitterswijk et al., 2013).

Transgene expression levels were examined in 19 lines carrying between 110 and 790 repeats (Figure 2F). Recognizing that transgenes with multiple repeat sizes would preclude correlation analyses of repeat-length- and expression-associated toxicity, we selected four lines with defined repeat lengths and/or different transgene expression levels: line 8 with ~110 repeats (hereafter designated C9¹¹⁰) and three lines expressing various levels of RNAs but each containing ~450 repeats (lines 1, 10, and 11, designated C9^{450A}, C9^{450B}, and C9^{450C}, respectively). C9¹¹⁰ and C9^{450B} have comparable levels of transgene expression but different repeat sizes, whereas C9^{450B} has a similar repeat size as C9^{450A}, but higher transgene expression (Figures 2C and 2F). *C9ORF72* transgene-encoded RNAs were three to four times the level of endogenous mouse *C9orf72* RNA in lines C9¹¹⁰, C9^{450B}, and C9^{450C}, and equal to endogenous *C9orf72* in line C9^{450A} (Figure 2G). Endogenous *C9orf72* RNAs were unchanged in all lines. Similar to total *C9ORF72* RNAs, repeat-containing RNAs (measured by qRT-PCR with variant-specific primers; Figure S3E) were higher in C9^{450B} mice than C9^{450A} mice. Repeat-containing RNAs were three times higher in C9¹¹⁰ than C9^{450B} mice (Figure 2H), despite comparable total *C9ORF72* RNA levels (Figures 2G and S3F). Breeding produced homozygous C9^{450C} mice with *C9ORF72* expression ~12 times the level of mouse *C9orf72* (Figures 2I and 2J).

Repeat Size- and Dose-Dependent Accumulation of Sense and Antisense RNA Foci

RNAs transcribed from both sense (GGGGCC) and antisense (GGCCCC) strands of *C9ORF72* have been reported to accumulate into RNA foci in cultured cells and postmortem tissues from C9ALS/FTD patients (Gendron et al., 2013; Lagier-Tourenne et al., 2013; Miziołinska et al., 2013; Zu et al., 2013). Use of fluorescence in situ hybridization detected sense and antisense foci in all three mouse lines expressing 450 repeats. Foci were found throughout the CNS, including the frontal cortex, hippocampus, cerebellum, and spinal cord, as early as 2 months of age (Figure 3A) and were not observed in wild-type mice (Figure S3G).

(B–D) Genomic DNA blot analysis of tail DNA from (B) founder (F0) and F1 transgenic mice from lines 9 or 15 and DNA from human fibroblasts (Hu) with normal *C9ORF72* alleles; (C) twelve different mice of lines 1, 8, 10, and 11 (redesignated C9^{450A}, C9¹¹⁰, C9^{450B}, and C9^{450C}, respectively); and (D) mice from F0, F2, and F5 generations in line C9^{450B}.

(E) Repeat lengths determined by genomic DNA blotting using DNA from the CNS and peripheral tissues of a C9^{450B} mouse.

(F) Human *C9ORF72* RNA in cortex of transgenic mice measured by qRT-PCR, normalized to C9^{450A} mice. Numbers above bars are repeat lengths measured by genomic DNA blots. Numbers in pink represent transgenes with different repeat lengths at the same locus that segregated together.

(G) Expression levels of total (human plus mouse) *C9ORF72* RNAs in the cortex of C9¹¹⁰, C9^{450A}, C9^{450B}, and C9^{450C} mice normalized to the level of endogenous *C9orf72* RNA.

(H) Level of repeat-containing *C9ORF72* RNA variants in the cortex measured by qRT-PCR and normalized to levels in C9^{450A} mice.

(I and J) Levels of (I) total *C9ORF72* RNAs (human plus mouse) normalized to *C9orf72* levels in wild-type littermates, or (J) repeat-containing *C9ORF72* RNA measured by qRT-PCR in the cortex of heterozygous and homozygous C9^{450C} mice. Error bars represent SEM from 3 to 5 biological replicates per group.

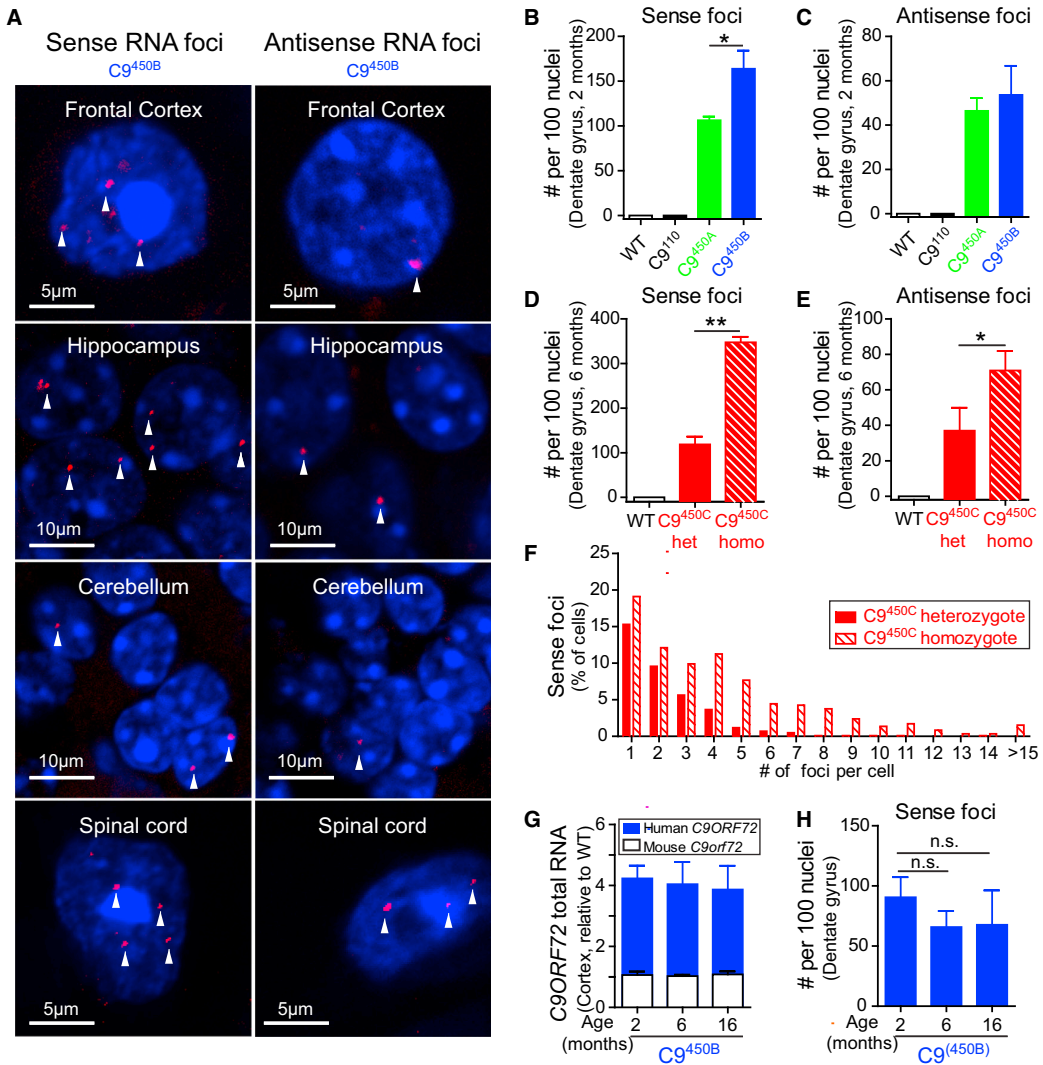


Figure 3. Repeat Size- and Dose-Dependent Accumulation of Sense and Antisense RNA Foci in *C9ORF72* Transgenic Mice

(A) FISH detection of sense and antisense RNA foci (arrows) in 2-month-old *C9^{450B}* mice. DNA was stained with DAPI.

(B–E) Numbers of sense and antisense foci (per 100 nuclei) in hippocampal dentate gyrus of (B and C) 2-month-old *C9¹¹⁰*, *C9^{450A}*, and *C9^{450B}* mice, and (D and E) 6-month-old heterozygous and homozygous *C9^{450C}* mice. Error bars represent SEM in 3–5 biological replicates. *p < 0.05, **p < 0.01 using Student's t test.

(F) Quantification of sense RNA foci per nucleus in hippocampal dentate gyrus of 6-month-old heterozygous and homozygous *C9^{450C}* mice.

(G) qRT-PCR measurement of human and mouse *C9ORF72* RNAs in cortex of 2-, 6-, and 16-month-old *C9^{450B}* mice, normalized to wild-type littermates (n = 2–4 per group).

(H) Numbers of sense foci (per 100 nuclei) in hippocampal dentate gyrus of 2-, 6-, and 16-month-old *C9^{450B}* mice. Error bars represent SEM in 2–4 biological replicates. n.s., not significant using one-way ANOVA.

Sense foci were most abundant in the frontal cortex, followed by the hippocampal dentate gyrus, retrosplenial cortex, and molecular layer of the cerebellum (Figure S3H). An unexpected, surprisingly strong influence of repeat length on foci formation was uncovered: whereas mice with 450 repeats developed foci (Figure 3A), neither sense nor antisense foci were detected in any brain region, or at any age, in *C9¹¹⁰* mice with 110 repeats (Figures 3B and 3C). This was despite the fact that transgene

expression in *C9¹¹⁰* mice was 3.5 times that of endogenous *C9orf72* RNAs (seven times the level of RNA from a single endogenous *C9orf72* allele) (Figure 2G) and that levels of repeat-containing RNAs in *C9¹¹⁰* mice were three and six times higher than in *C9^{450B}* and *C9^{450A}* mice, respectively (Figure 2H).

Doubling the level of 450 repeat-containing sense strand RNAs (compare RNA levels in *C9^{450B}* versus *C9^{450A}*, Figures 2G and 2H) doubled sense foci accordingly (Figure 3B). Similarly,

doubling repeat-containing RNAs by generating homozygous C9^{450C} mice more than doubled the overall number of sense foci (Figure 3D) and the number of foci per cell (Figure 3F). The proportion of cells that developed sense foci also increased from 52% in the dentate gyrus of heterozygous C9^{450C} mice to 81% in homozygous mice (Figure S3I), and some cells accumulated more than 30 sense foci (Figure 3F). Transgene expression and foci burden remained constant with age (Figures 3G and 3H).

Antisense RNAs from the human C9ORF72 transgene, identified using a strand-specific RT-PCR strategy (Figures S3K and S3L), also accumulated into RNA foci (Figure 3A). As with sense foci, antisense foci increased with increased repeat length (Figure 3C) and RNA expression level, with both the overall number of antisense foci (Figure 3E) and the percentage of cells with foci (Figures S3I and S3J) nearly doubling in homozygous versus heterozygous C9^{450C} mice.

Age-, Repeat-Length-, and Expression-Dependent Cytoplasmic Inclusions of DPR Proteins

Inclusions of DPR proteins produced by RAN translation from GGGGCC or GGCCCC repeats are a neuropathological hallmark of C9ALS/FTD (Ash et al., 2013; Gendron et al., 2013; Mori et al., 2013a, 2013c; Zu et al., 2013). As in human patients, perinuclear, cytoplasmic aggregates of sense strand RNA-encoded poly(GA), poly(GP), or poly(GR) proteins were detected in multiple CNS regions in C9^{450C} mice as young as 3 months of age (Figures 4A and 4B). Poly(GA) and poly(GP) aggregates in 22-month-old C9^{450C} mice were most abundant in the retrosplenial cortex, followed by the hippocampal dentate gyrus and frontal cortex (Figures 4C and S4A). Fewer poly(GA) aggregates were observed in the cerebellum (Figure S4B) or spinal cord. Dot blot assay confirmed accumulation of poly(GP) in cortical lysates from 6-month-old C9^{450C} mice (Figure S4C). As in C9ALS/FTD patients (Mori et al., 2013a), DPR proteins coaggregated into common, p62-containing inclusions (Figures 4D, 4E, and S4D). Antisense strand-encoded poly(PR) and poly(PA) proteins have only been detected in rare aggregates in patient samples (Gendron et al., 2013; Mackenzie et al., 2015; Mori et al., 2013a; Schludi et al., 2015; Zu et al., 2013). None were detected in C9 mice of any line or at any age.

Similar to RNA foci formation, DPR protein expression was dependent on repeat length, as established by immunoassay for quantitative measurements of poly(GP) (Su et al., 2014). Although C9¹¹⁰ mice expressed a 3-fold higher level of repeat-containing C9ORF72 RNAs than C9^{450B} mice (Figure 2H), no poly(GP) was detected in 2% SDS-soluble homogenates prepared from tissues of various neuroanatomical regions from C9¹¹⁰ mice, while poly(GP) was easily detected in mice expressing 450 repeats (Figure 4F). As expected, more poly(GP) was detected in mice with higher C9ORF72 RNA expression (compare C9^{450A} and C9^{450B} mice; Figure 4F; and homozygous C9^{450C} versus age-matched heterozygotes; Figure 4G).

SDS-soluble poly(GP) decreased with age in C9^{450A} and C9^{450B} mice (Figure 4H), despite constant transgene expression (Figure 3G), indicating that DPR proteins may become insoluble over time. Consistent with this notion, poly(GA) aggregated more in the retrosplenial cortex (Figure 4I) and hippocampus (Fig-

ure S4E) as mice aged, and the size of poly(GA) inclusions increased over time (Figure 4J). Age-dependent increases in the number and size of poly(GP) and poly(GR) aggregates were also detected (Figures S4F and S4G). In addition, more cells accumulated DPR protein aggregates in 3-month-old C9^{450C} homozygous mice compared to heterozygous mice, and the abundance of such aggregates was increased at 6 months of age (Figures 4I, 4K, S4F, and S4G).

Age-Dependent Cognitive Impairment in C9 Mice Expressing 450 Repeats

C9 transgenic mice were tested for age-dependent disease. No significant motor deficits or weight loss were observed by 18 months of age in two mouse lines expressing 450 repeats (C9^{450B} or C9^{450C}; Figures 5A–5C, S5A, and S5B). By 12 months of age, no loss of ChAT-positive lower motor neurons (Figures 5D and 5E) or increased glial activation (Figure S5C) was detected in the spinal cord of C9^{450C} mice, which express the highest levels of transgene. Functional innervation and connectivity of the entire neuromuscular unit were normal, as measured by resting EMG recordings and MMEP amplitudes, respectively, in 12-month-old C9¹¹⁰ and C9^{450C} mice (Figures S5D and S5E). There was no loss of CTIP-2-positive upper motor neurons in layer 5 of the motor cortex in either line (Figure S5F).

Cognitive and behavioral dysfunction, however, developed in an age-dependent manner. While 4-month-old C9^{450B} mice performed as well as wild-type littermates in an assay that measures spatial learning and memory (the Barnes maze), both C9^{450B} and C9^{450C} lines developed deficits by 12 months of age that were sustained to 18 months (Figure 6A). A second spatial-learning assay (the radial arm maze) confirmed a working memory deficit at 12 and 18 months of age in C9^{450B} and C9^{450C} mice (Figure 6B). Aged C9^{450B} and C9^{450C} male mice also displayed abnormalities in two “anxiety” assays, a marble burying test (Figure 6C) and an elevated plus maze (Figure 6D). The spatial learning and anxiety abnormalities were not accompanied by behavioral differences in social interaction, social recognition, or social communication, nor did assays of novel object recognition, fear conditioning, and serial reversal learning uncover any impairment (Figures S6C–S6H).

Recognizing the crucial role of the hippocampus in spatial learning and memory (Sharma et al., 2010), we tested the C9 mice for age-dependent hippocampal neuron loss. Blinded quantification in two hippocampal regions (the dentate gyrus and CA1 region) of 4- and 12-month-old C9^{450B} and C9^{450C} mice identified mild, age-dependent neuronal loss (Figures 6E and 6F). Neuronal loss was repeat-length dependent, as no loss was seen in C9¹¹⁰ mice that expressed higher levels of repeat-containing RNAs than C9^{450C} mice (Figure S7A). No astrogliosis or microgliosis was observed, and neuronal loss was region specific, as the neuronal density in the retrosplenial cortex remained unchanged (Figure S7A). Although levels of both sarkosyl-soluble and sarkosyl-insoluble (but urea-soluble) phosphorylated TDP-43 (pTDP-43) were significantly increased in 22-month-old C9^{450C} mice (Figure S7C), no TDP-43 mislocalization or aggregation was observed (Figure S7B). Similarly, no mislocalized, discontinuous, or punctate aggregates of RanGAP1 or Lamin B (Figures S7D and S7E) were identified.

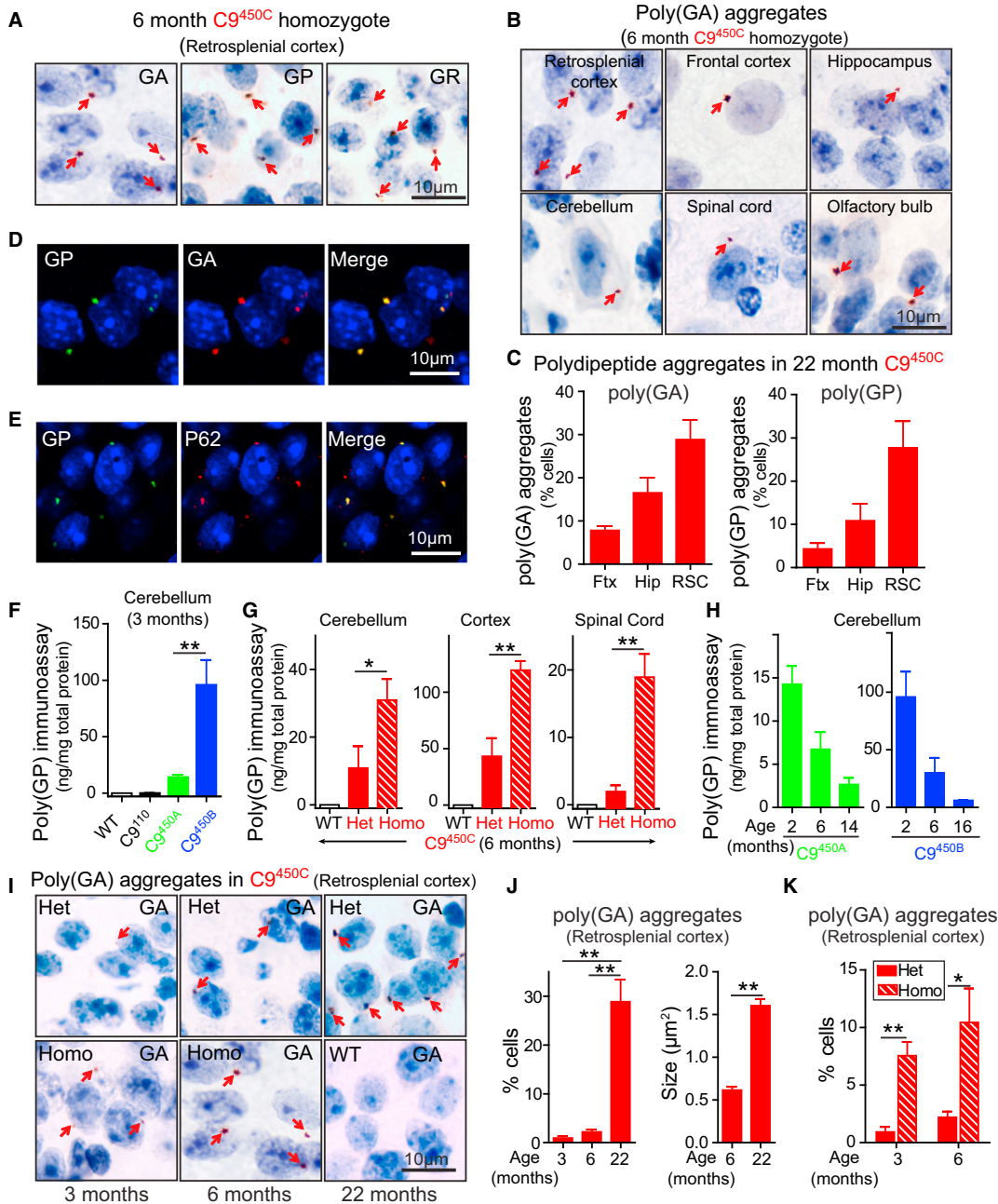


Figure 4. Repeat Size- and Expression-Dependent Production of Sense-Strand-Encoded DPR Proteins Is Associated with Age-Dependent Formation of Cytoplasmic Inclusions

(A) Poly(GA), poly(GP), and poly(GR) perinuclear aggregates (arrows) detected by immunohistochemistry in the retrosplenial cortex of 6-month-old homozygous $C9^{450C}$ mice. Nuclei were stained with haemalum.

(B) Poly(GA) aggregates (arrows) in different CNS regions of 6-month-old homozygous $C9^{450C}$ mice.

(C) Percent of cells containing poly(GA) or poly(GP) inclusions in frontal cortex (Ftx), hippocampus (Hip), and retrosplenial cortex (RSC) of 22-month-old heterozygous $C9^{450C}$ mice (n = 2–4 biological replicates).

(D and E) (D) Aggregates positive for (green) poly(GP), (red) poly(GA), or (yellow) both, and (E) (green) poly(GP) and (red) P62-positive inclusions identified by immunofluorescence in retrosplenial cortex of 6-month-old homozygous $C9^{450C}$ mice. DNA is stained with DAPI.

(legend continued on next page)

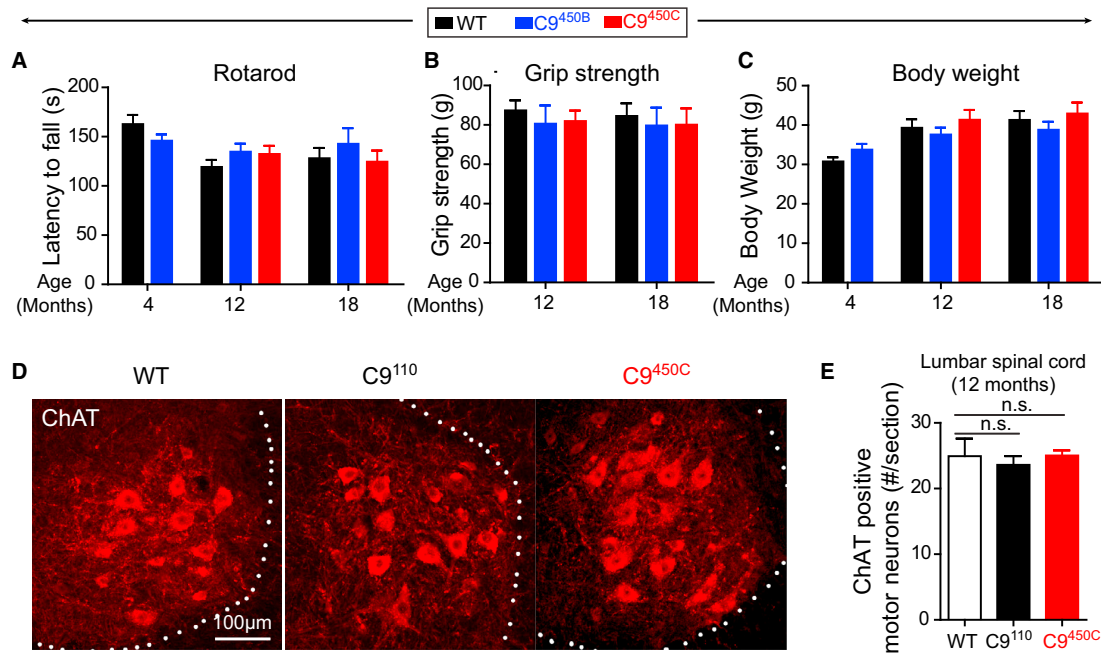


Figure 5. No Motor Neuron Loss and Motor Deficits in C9ORF72 Transgenic Mice with 450 Repeats

(A–C) (A) Motor performance on a rotarod measured by latency to fall, (B) hindlimb grip strength, and (C) body weight of 4-, 12-, and 18-month-old wild-type (WT), C9^{450B}, and C9^{450C} mice. (D) Choline acetyltransferase (ChAT)-positive motor neurons detected by immunofluorescence in the anterior horn of lumbar spinal cord of 12-month-old WT, C9¹¹⁰, and C9^{450C} mice. (E) Average number of ChAT-positive neurons per section. Error bars represent SEM in $n = 4\text{--}5$ animals per group. n.s., not significant using one-way ANOVA.

Single-Dose ASOs Reduce Foci, DPR Proteins, and Behavioral Deficits in C9 Mice

ASOs mediate cleavage of target RNAs through action of the primarily nuclear enzyme RNase H, and ASO therapy has gone to clinical trial for ALS (Miller et al., 2013; Smith et al., 2006) and at least two neurodegenerative disorders linked to repeat expansions: myotonic dystrophy (Wheeler et al., 2012) and Huntington's disease (Kordasiewicz et al., 2012). To test whether *in vivo* administration of ASOs can mediate RNase H-dependent, selective reduction of C9ORF72 hexanucleotide repeat-containing RNAs in the rodent CNS, 3-month-old C9^{450B} mice were treated with a single intraventricular bolus injection of ASOs targeting human C9ORF72 RNAs or a control ASO that does not have any target in the mouse genome (Figure 7A). One C9ORF72 ASO (ASO1) was complementary to a sequence that partially overlaps the 5' end of the hexanucleotide expansion and specifically targets repeat-containing C9ORF72 RNA variants. A sec-

ond ASO (ASO2) hybridizes within exon 2 and thus targets all C9ORF72 RNA variants (Figure 7B). Four weeks after a single injection, both ASO1 and ASO2 decreased repeat-containing C9ORF72 RNA levels in the cortex and spinal cord to 20%–40% of levels in control ASO-treated mice (Figure 7C). As expected, ASO2 decreased total and exon 1b-containing C9ORF72 RNAs by 40%–60%. However, ASO1, which targets repeat RNA, preserved exon 1b-containing, C9ORF72 protein-encoding RNAs (Figure 7E) and 80% of total C9ORF72 RNAs (Figure 7D).

Within 4 weeks after a single injection of either ASO1 or ASO2, the number of sense foci was reduced to 40%–45% (Figures 7F and 7G). Antisense RNA foci remained unchanged (Figure 7F). Both SDS-soluble poly(GP) and poly(GA) were decreased to almost undetectable levels in the cortex and spinal cord (Figures 7H and 7I). The profound reduction of poly(GP), which can be translated from sense or antisense strand RNAs, demonstrates

(F–H) Levels of poly(GP) soluble in 2% SDS measured by immunoassay in (F) cerebellum of 3-month-old C9¹¹⁰, C9^{450A}, and C9^{450B} mice; (G) cerebellum, cortex, and spinal cord of 6-month-old heterozygous and homozygous C9^{450C} mice; and (H) during aging in the cerebellum of C9^{450A} and C9^{450B} mice ($n = 2\text{--}5$ biological replicates).

(I) Poly(GA) aggregates (arrows) identified by immunohistochemistry in retrosplenial cortex of heterozygous or homozygous C9^{450C} mice or wild-type mice at the noted ages.

(J) (Left panel) Percent of cells containing poly(GA) aggregates and (right panel) average size of poly(GA) inclusions in retrosplenial cortex of C9^{450C} mice ($n = 2\text{--}3$ biological replicates).

(K) Percent of cells with poly(GA) inclusions in retrosplenial cortex of heterozygous and homozygous C9^{450C} mice ($n = 3$ per group). Error bars represent SEM.

* $p < 0.05$, ** $p < 0.01$ using Student's t test.

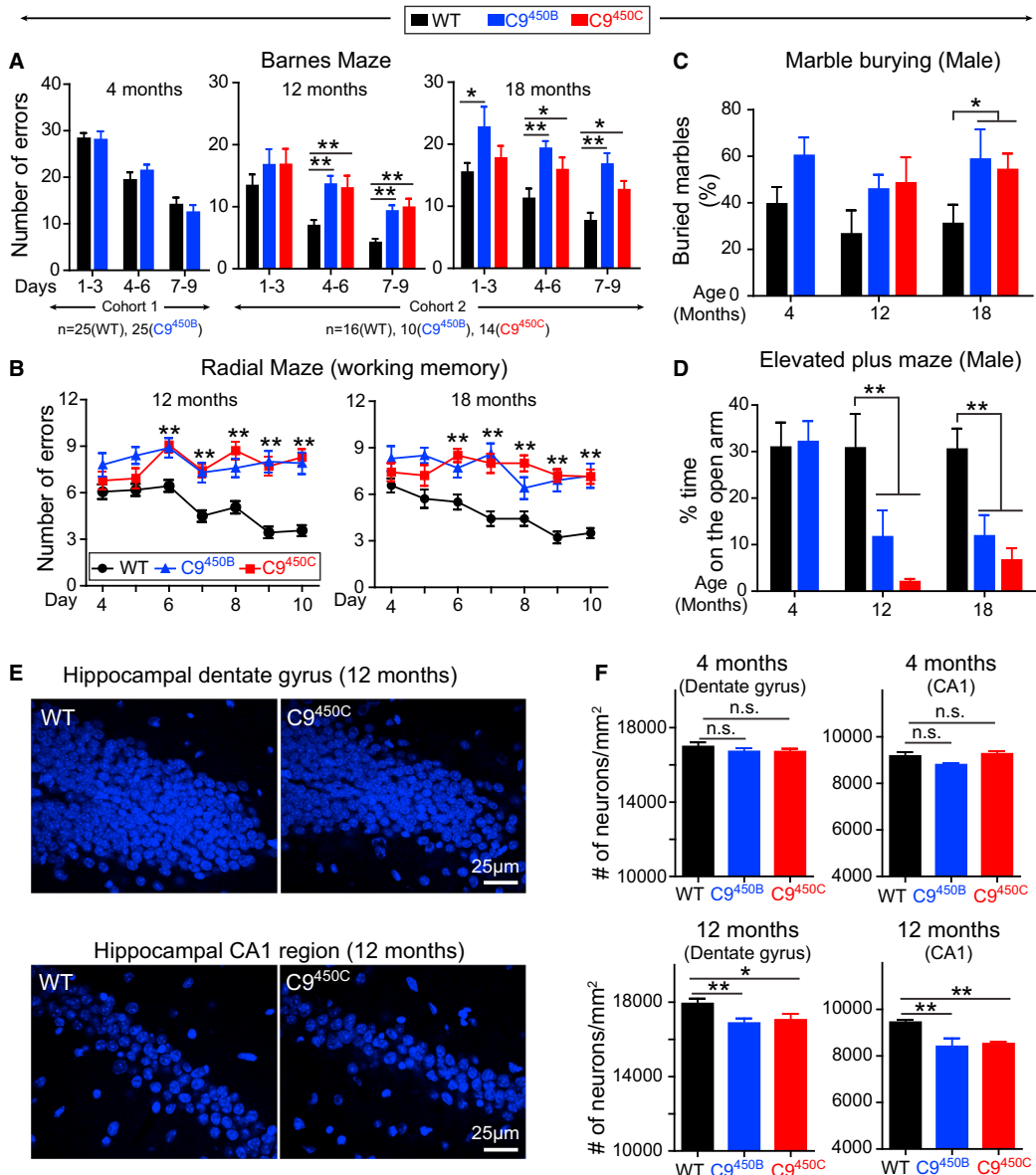


Figure 6. Age-Dependent Increased Anxiety and Impaired Cognitive Function in C9ORF72 Mice with 450 Repeats

(A and B) Behavioral performances in WT, C9^{450B}, and C9^{450C} mice at 4, 12, and 18 months of age ($n = 25$ mice per group at 4 months and $n = 16$ [WT], $n = 14$ [C9^{450B}], and $n = 10$ [C9^{450C}] at 12 and 18 months of age). (A) Spatial learning and memory performance on a Barnes maze showing the number of errors in finding the escape chamber at days 1–3, 4–6, and 7–9. (B) Working memory performance on a radial maze showing errors per trial over 10 days of testing. (C and D) Anxiety-related behaviors in WT, C9^{450B}, and C9^{450C} male mice at 4, 12, and 18 months of age ($n = 11$ [WT] and $n = 13$ [C9^{450B}] at 4 months, and $n = 9$ [WT], $n = 4$ [C9^{450B}], and $n = 7$ [C9^{450C}] at 12 and 18 months of age). (C) Anxiety-related behavior determined by marble burying test showing the percent of marbles buried during a 20 min trial, and (D) elevated plus maze showing the percent of time spent on the open arm. (E and F) (E) Representative images and (F) quantification of DAPI-positive nuclei in the hippocampal dentate gyrus and CA1 region in 4- and 12-month-old WT, C9^{450B}, and C9^{450C} mice ($n = 4$ –5 per group). Error bars represent SEM, n.s., not significant, * $p < 0.05$ and ** $p < 0.01$ using one-way ANOVA.

that in our transgenic mice, poly(GP) proteins are mostly translated from sense strand RNAs.

Selective reduction of repeat-containing RNAs with attenuated RNA foci and RAN translation was confirmed by single-

dose injection of two additional ASOs (ASO3 and ASO4) targeting sequences 5' to the expansion within C9ORF72 intron 1 (Figures 7B and S8A). Two weeks after treatment, repeat-containing C9ORF72 RNAs in cortex and spinal cord were reduced

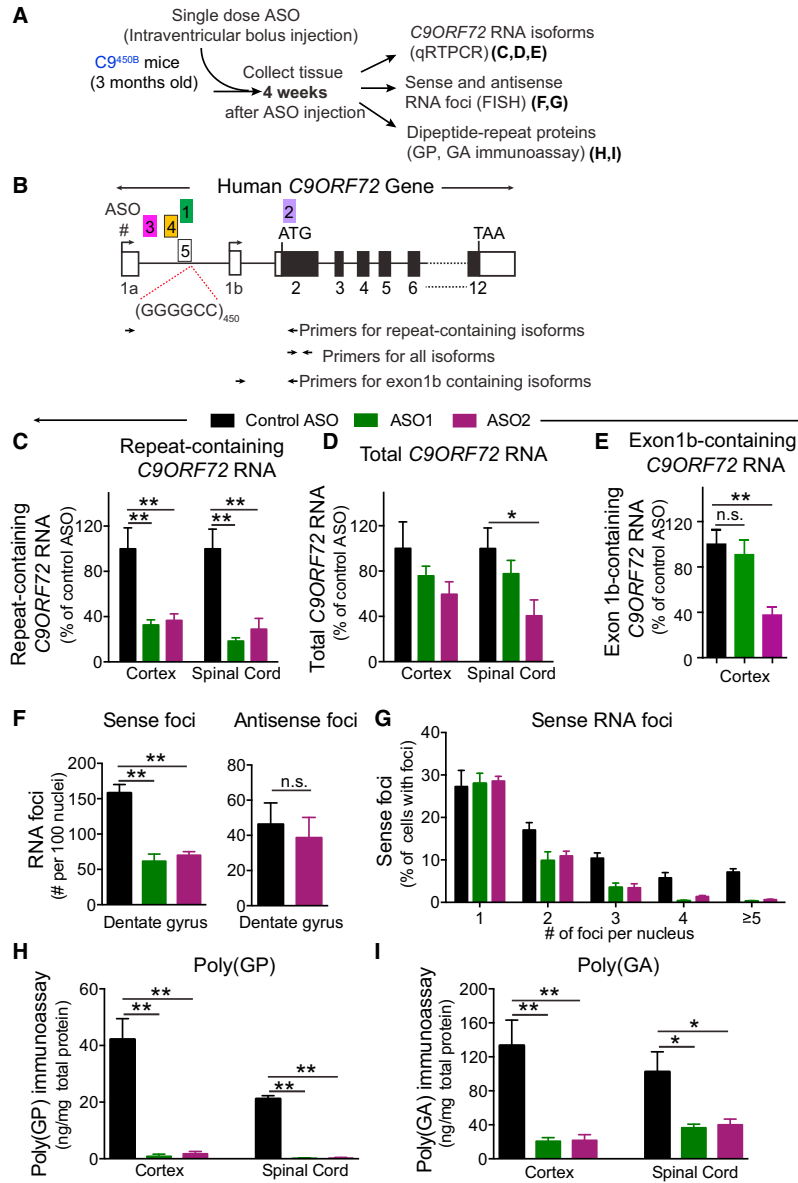


Figure 7. Sustained Reduction in RNA Foci and DPR Proteins from a Single Dose of ASOs Targeting C9ORF72 Repeat-Containing RNAs

(A) Schematic of injected ASOs targeting the sense strand C9ORF72 transcripts for degradation in 3-month-old C^{450B} mice.

(B) Schematic of the C9ORF72 gene showing the GGGGCC repeats within the first intron, the two transcription initiation sites (arrows), the positions of five ASOs, and primers for detection (by qRT-PCR) of various C9ORF72 RNAs.

(C–E) Expression of (C) repeat-containing, (D) total, and (E) exon 1b-containing C9ORF72 RNAs determined by qRT-PCR in mice treated either with ASO1 targeting only the repeat-containing RNAs, ASO2 targeting all C9ORF72 variants, or a control ASO.

(F and G) (F) Number of sense and antisense foci (per 100 nuclei) determined by FISH and (G) quantification of sense foci per nucleus in hippocampal dentate gyrus.

(H and I) Levels of (H) poly(GP) or (I) poly(GA) in the cortex and spinal cord of C^{450B} mice treated with ASO1, ASO2, or a control ASO, as measured by immunoassay. Error bars represent SEM in n = 5–6 biological replicates. *p < 0.05, **p < 0.01, n.s. not significant using one-way ANOVA.

to 40% of a PBS-treated group, with total C9ORF72 RNAs remaining at 80% of their initial level (Figures S8B and S8C). Sense foci were reduced by half; antisense foci were unaffected. SDS-soluble poly(GP) levels were reduced by more than 80% in cortex and 50% in spinal cord (Figure S7D), and poly(GP) aggregates, quantified in a blinded fashion, were significantly decreased in ASO3- or ASO4-treated mice (Figures S8E and S8F). Thus, intron 1-targeting ASOs rapidly decrease both soluble and insoluble DPR proteins throughout the mouse CNS.

Finally, 9-month-old C^{450B} mice were injected with an ASO targeted to repeat-containing RNAs (Figure 8A). Repeat-containing C9ORF72 RNAs in the cortex and spinal cord were sharply

reduced (to 23% and 12% of control levels, respectively) within 2 weeks of treatment (Figure 8B). Consistent with our assays with an independent cohort (Figures 6A–6D), C^{450B} mice injected with a control ASO developed increased anxiety (in marble burying test and elevated plus maze) and impaired cognition (in Barnes and radial mazes) (Figures 8C–8F). Single-dose ASO injection at 9 months alleviated these age-dependent deficits (Figures 8C–8F). In fact, at 15 months (6 months after injection), the beneficial effects were sustained, with a trend suggestive of further improvement. Correspondingly, SDS-soluble poly(GP) and poly(GA) levels remained lower in 16-month-old mice treated with the repeat-targeting ASO (Figure 8H), even

though repeat-containing C9ORF72 RNA levels had recovered to their initial level (Figure 8G).

DISCUSSION

A key question regarding pathogenic mechanisms in C9ALS/FTD has been whether the repeat expansion causes disease through loss of C9ORF72 function, gain of toxicity from repeat RNA, or both. By producing and analyzing mice with a chronic reduction of C9ORF72 or that express the human C9ORF72 gene with different sizes of expanded repeats, we have identified gain of toxicity as a central disease mechanism in a mammalian

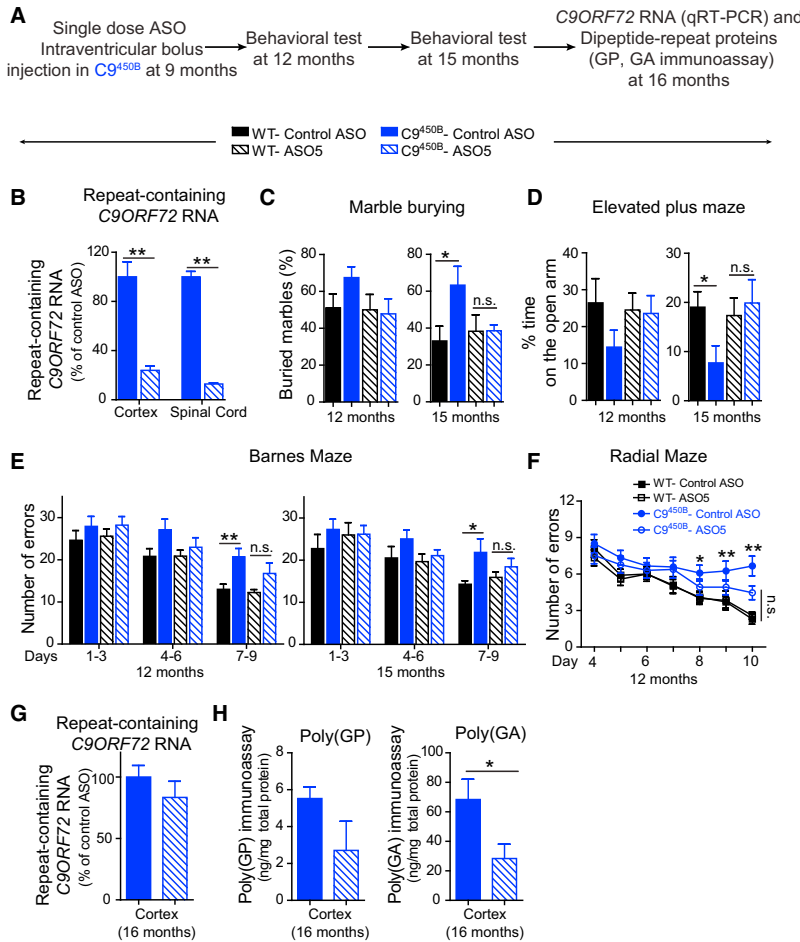


Figure 8. Single-Dose ASO Treatment Alleviates Age-Dependent Behavioral Deficits in C9ORF72 Mice Expressing 450 Repeats

(A) Schematic of the experimental procedure for a single-dose ASO targeting degradation of the sense strand C9ORF72 RNA in 9-month-old C9^{450B} mice.

(B) Expression of repeat-containing C9ORF72 RNAs was determined by qRT-PCR 2 weeks after injection of ASO5 or control ASO ($n = 6$ per group).

(C and D) Anxiety-related behaviors determined by (C) marble burying test and (D) elevated plus maze in 12- and 15-month-old WT and C9^{450B} mice treated with either control ASO or ASO5 ($n = 5$ –7 per group).

(E and F) Cognition-related behaviors determined on (E) a Barnes maze and (F) a radial maze in 12- and 15-month-old WT and C9^{450B} mice treated with either control ASO or ASO5 ($n = 10$ –13 per group).

(G and H) Expression of repeat-containing C9ORF72 RNAs and (H) levels of poly(GP) or poly(GA) proteins in the cortex of 16-month-old C9^{450B} mice treated at 9 months with ASO5 or control ASO. Error bars represent SEM in biological replicates. * $p < 0.05$, ** $p < 0.01$, n.s. not significant, using Student's t test.

nervous system. Mice expressing RNAs with 450 repeats from two independent lines developed age-dependent, anxiety-like behavior and impaired cognitive function by 12 months of age, accompanied by mild hippocampal neuronal loss. In contrast, mice hemizygous for C9ORF72 that express 50% of C9orf72 mRNA, as observed in C9ALS/FTD patients (DeJesus-Hernandez et al., 2011; Gajdusek et al., 2012; van Blitterswijk et al., 2015), did not develop an ALS/FTD-like phenotype or any other phenotype in the CNS or periphery. Hence, by a systematic comparison of multiple mouse lines, we now demonstrate that reduction of C9ORF72 expression is not sufficient to trigger neurodegeneration in mice, while pathological hallmarks of C9ALS/FTD, neuronal loss and cognitive dysfunction develop in mice expressing expanded repeat RNA.

The function of the 54 kD C9ORF72 protein has not been established, but its sequence homology to the DENN protein family predicts a possible role in regulating membrane trafficking (Farg et al., 2014; Levine et al., 2013; Zhang et al., 2012). The C9orf72 gene is expressed not only in the CNS but also in peripheral tissues, including spleen (Suzuki et al., 2013), bone marrow, lymphocytes, and macrophages (BioGPS data; <http://biogps.org/>).

By disrupting both C9orf72 alleles, we determined that complete elimination of C9ORF72 from mice produces splenomegaly, enlarged cervical lymph nodes, and premature death. While loss of C9ORF72 during embryonic development has been reported to produce motor deficits in zebrafish (Ciura et al., 2013) and *C. elegans* (Therrien et al., 2013), systemic (our work here and

Atanasio et al., 2016; O'Rourke et al., 2016) or nestin-cre (Koppes et al., 2015)-mediated ablation of C9orf72 in mice is not associated with motor degeneration, defects in motor function, or altered survival. In addition, no loss-of-function mutations in C9ORF72, including nonsense or frameshift mutations, have been linked to ALS or FTD (Harms et al., 2013), and reduced expression of expanded RNAs following hypermethylation of the C9ORF72 promoter may actually be neuroprotective (Liu et al., 2014; McMillan et al., 2015; Russ et al., 2015). While our studies reinforce conclusions that C9ORF72 plays an important role in immune cells (Atanasio et al., 2016; O'Rourke et al., 2016), chronic reduction of C9ORF72 alone is not sufficient to cause ALS/FTD symptoms in mice. A key remaining question, now testable with the mice we report here, is whether a reduction in C9ORF72 synergizes with repeat-mediated gain of toxicity to potentiate disease.

Our analysis uncovered an unexpected association between hexanucleotide repeat length and accumulation of RNA foci and DPR proteins. When expressed at seven times the level of an endogenous C9orf72 allele, no detectable DPR proteins accumulate in mice expressing 110 repeats (Figure 4F). Conversely,

mice with lower RNA levels but with 450 repeats produce both soluble DPR proteins (Figures 4F–4H) and insoluble aggregates (Figures 4I–4K). That no DPR proteins were detected in C9¹¹⁰ mice could be due to (1) RAN translation initiation of short repeats being less efficient than of long repeats; (2) shorter DPR proteins having shorter half-lives than longer DPR proteins; (3) shorter repeat-containing RNAs being less effectively transported to the cytoplasm, the presumed site of RAN translation; or (4) a combination of options 1–3.

While a prior study demonstrated that robust adeno-associated-virus-mediated expression of 66 GGGGCC repeats led to the aggregation of DPR proteins throughout the murine CNS (Chew et al., 2015), we demonstrate here that expression of a short repeat does not generate such pathology in mouse brain when expressed at seven times the levels of RNA from a single *C9orf72* allele. Not only do long and short repeats have differing capacities to generate DPR proteins, long and short DPR proteins have different intracellular localization and aggregation profiles. For instance, DPR proteins translated from 66 repeats produced a level of accumulated poly(GP) that reached 1.8% of total brain protein by 6 months of age and formed primarily nuclear aggregates (Chew et al., 2015), whereas we and others (O'Rourke et al., 2015; Peters et al., 2015) have shown that in mice with 400–500 repeats, DPR proteins form cytoplasmic inclusions similar to those observed in C9ALS/FTD patients. Short DPR proteins are likely to be more soluble and sufficiently small to freely diffuse through nuclear pores, thereby facilitating the intranuclear aggregation of DPR proteins seen in mice expressing 66 repeats (Chew et al., 2015). Similarly, the nucleolar disruption and acute toxicity resulting from exposing cultured cells to 10 μM of 20-mer poly(PR) or poly(GR) proteins (Kwon et al., 2014) differ markedly from the primarily cytoplasmic aggregates observed in mice expressing 450 repeats and C9ALS/FTD patients (Ash et al., 2013; Gendron et al., 2013; Mackenzie et al., 2015; Mori et al., 2013a; Zu et al., 2013).

While the minimal pathogenic repeat size in *C9ORF72* patients is not established, somatic expansion can take the germline-transmitted repeat to 3,000–5,000 repeats in the most affected brain regions (Gijsselinck et al., 2015; van Blitterswijk et al., 2013). We have found minimal somatic expansion in either the CNS or peripheral tissues of mice. Also differing from C9ALS/FTD patients, our C9⁴⁵⁰ mice did not display TDP-43 mislocalization or aggregation, although increased levels of phosphorylated TDP-43 were detected. In addition, we did not observe mislocalization of proteins involved in nucleocytoplasmic transport. Lack of these features may explain the relatively mild phenotype observed in our transgenic mice despite expression of up to 24 times a single endogenous *C9orf72* allele. While abundant RNA foci did not increase with age in our mice, an age- and repeat-length-dependent increase in the number and size of cytoplasmic DPR aggregates was seen, with soluble poly(GP) levels decreasing with age (Figure 4H). In C9ALS/FTD, the anatomical distribution of DPR protein pathology does not correlate with neurodegeneration (Schludi et al., 2015). These findings suggest that certain neuroanatomical regions are less susceptible to DPR proteins, or that soluble DPR proteins are toxic and DPR protein aggregates are neuroprotective. In support of the latter, poly(GA) can recruit poly(GR) into inclusions and partially

decrease poly(GR) toxicity in *Drosophila* and cultured cell models (Yang et al., 2015). On the other hand, aggregation of poly(GA) was recently reported to be necessary for its toxicity, which is mediated through sequestration of HR23 and nucleocytoplasmic transport proteins (Zhang et al., 2016).

Despite uncertainty about the contributions of RNA foci or DPR proteins to neurodegeneration, an “on mechanism” therapy would be one that reduces repeat-containing RNAs, thereby attenuating both potential toxicities. We have established the potency of multiple ASOs for selective reduction of repeat-containing *C9ORF72* RNAs in the mammalian CNS while having minimal effect on total *C9ORF72* RNAs. Importantly, single-dose ASO (1) significantly mitigated the accumulation of sense RNA foci (without increasing antisense foci) and of poly(GP) and poly(GA) proteins and (2) significantly attenuated the development of behavioral deficits even 6 months after treatment. Thus, our studies establish a repeat-dependent gain of toxicity as a crucial pathological mechanism of C9ALS/FTD and, most importantly, validate the feasibility of employing ASO therapy to mitigate the toxicity from repeat RNAs without exacerbating a potential loss of *C9ORF72* function.

EXPERIMENTAL PROCEDURES

Please see the [Supplemental Experimental Procedures](#) for more information

Generation of *C9ORF72* BAC Transgenic Mice

The human BAC construct expressing a truncated *C9ORF72* gene with 450 repeat expansions was obtained from BACPAC resource center at Children's Hospital Oakland Research Institute (clone ID: CH523-111K12) and was injected into the pronuclei of fertilized C57BL/6/C3H hybrid eggs and implanted into pseudo-pregnant female mice. Mice used in this report were then back-crossed to C57BL/6 for a minimum of three generations. All experimental procedures were approved by the Institutional Animal Care and Use Committee of the University of California, San Diego.

RNA Extraction and qRT-PCR

Procedures are detailed in the [Supplemental Information](#). Primers and probe sequences are listed in [Table S1](#).

Generation of Antibodies Recognizing DPR Proteins

Peptide antigens (C-Ahx-(GA)8-amide, C-Ahx-(GR)8-amide, C-Ahx-(PR)8-amide, C-Ahx-(GP)8-amide, and C-Ahx-(PA)8-amide) were used to immunize rabbits to generate antibodies against DPR proteins. Pre-immune serum from each rabbit was tested using peptide antigens and tissue from C9ALS/FTD cases by immunoblot and immunohistochemistry, respectively, and confirmed negative. Antiserum or affinity-purified antibodies were used. Antibodies specific for each DPR protein are herein annotated Rb4333 poly(GA), Rb4335 poly(GP), Rb4995 poly(GR), Rb15898 poly(PA), and Rb15986 poly(PR).

Immunofluorescence Staining and X-gal Staining

Sections from paraformaldehyde-fixed tissues were stained using standard protocols with antibodies against GFAP (Chemicon, 1:1000), IBA1 (Wako, 1:500), ChAT (Millipore, 1:300), NeuN (GeneTex, 1:1000), CTIP2 (Abcam, 1:500), poly(GA) (Rb4333, 1:1000), poly(GP) (Rb4335, 1:1000), poly(GR) (Rb4995, 1:1000), poly(PR) (Rb15986, 1:100), poly(PA) (Rb15989, 1:100), TDP-43 (Proteintech, 1:500), RanGAP1 (Santa Cruz, 1:500), Lamin B (Santa Cruz, 1:20,000), and P62 (Abnova, 1:100). Confocal images were acquired on a Nikon Eclipse laser scanning confocal microscope using the Nikon EZ-C1 software. LacZ activity was assessed with X-gal staining solution (1.0 mg/mL of X-gal, 5 mM potassium ferrocyanide, and 2 mM MgCl₂) for 12 hr at 37°C. The sections were examined and photographed with a Nanozoomer.

Injection of ASO in the Mouse CNS

Intra-cerebroventricular (ICV) stereotactic injections of 10 μ L of ASO solution, corresponding to a total of 350 μ g of ASOs (Ionis Pharmaceuticals), were administered into the right ventricle using the following coordinates: 0.2 mm posterior and 1.0 mm lateral to the right from the bregma and 3 mm deep. Mice were treated either with PBS; a control ASO; ASOs targeting total *C9ORF72* (ASO2); or repeat-containing *C9ORF72* variants (ASO1, ASO3, ASO4, or ASO5). The sequences of the ASOs are available in Table S2.

SUPPLEMENTAL INFORMATION

Supplemental Information includes Supplemental Experimental Procedures, eight figures, and two tables and can be found with this article online at <http://dx.doi.org/10.1016/j.neuron.2016.04.006>.

AUTHOR CONTRIBUTIONS

J.J., Q.Z., T.F.G., P.J., S. Sabre, S.-C.L., M.M., C.J.H., P.V.D., D.T.U., A.D., S.M.H., L.P., C.F.B., S.D.C., J.R., F.R., D.W.C., and C.L.-T. designed the experiments and analyzed the data. J.J., Q.Z., T.F.G., S. Sabre, J.E.S., P.J., K.D., S.C., A.S., S. Sun, S.-C.L., M.M.-D., B.M., J.E., M.K., M.B., O.P., A.W., C.J.H., L.D.M., L.M.D., A.D., and D.T.U. performed the experiments. M.C.A., D.S., D.A.S., L.T., C.J.J., P.J.D.J., D.E., S.M.H., and C.E.S. contributed key reagents and methodology. J.J., Q.Z., T.F.G., D.W.C., and C.L.-T. wrote the manuscript.

ACKNOWLEDGMENTS

We thank Patrick King, Clement Ng, Cheyenne Schloffman, Marcus Maldonado, Anh Bui, and Drs. Ricardos Tabet, Kent Osborn, and Nissi Varki for their advice and technical assistance. We thank all members of D.W.C., C.L.-T., and J.R. groups and the team at Ionis Pharmaceuticals for critical suggestions on this project. This work was supported by the ALS Association (a Neurocollaborative grant to D.W.C., grants to T.F.G. and L.P., and a Milton Safenowitz postdoctoral fellowship to Q.Z.); grants from the NIH (R01-NS088578 to J.R. and D.W.C., R01-NS087227 to C.L.-T., R21-NS089979 to T.F.G., as well as R21-NS084528, R01-NS088689, R01-NS063964, R01-NS077402, and P01-NS084974 to L.P.); the UCSD Alzheimer's Disease Research Center (to C.L.-T.); research project funding from Target ALS to C.L.-T. (13-04827), J.R. (13-44792), and L.P.; the Robert Packard Center for ALS Research at Johns Hopkins (to L.P.); the Mayo Clinic Foundation (to L.P.); a senior clinical investigatorship and a grant from FWO-Vlaanderen to P.V.D.; the Belgian Alzheimer Disease Association (SAO); to P.V.D.); and the European Union's Seventh Framework Programme FP7/2014-2019 under grant agreement n° 617198 [DPR-MODELS] (to D.E.). J.J. was supported by NIH postdoctoral fellowships (T32 AG00216 and F32 NS087842). S. Sun is the recipient of career development grants from the NIH (K99 NS091538) and Target ALS. L.D.M. is employed by Janssen Pharmaceutical Companies of Johnson & Johnson. P.J., S.C., J.E., A.W., C.F.B., and F.R. are employees and D.W.C. is a consultant for Ionis Pharmaceuticals. J.R. received salary support from the University of California, San Diego. C.L.-T. and D.W.C. received salary support from the Ludwig Institute for Cancer Research.

Received: December 22, 2015

Revised: February 29, 2016

Accepted: April 4, 2016

Published: April 21, 2016

REFERENCES

- Ash, P.E., Bieniek, K.F., Gendron, T.F., Caulfield, T., Lin, W.L., DeJesus-Hernandez, M., van Blitterswijk, M.M., Jansen-West, K., Paul, J.W., 3rd, Rademakers, R., et al. (2013). Unconventional translation of *C9ORF72* GGGGCC expansion generates insoluble polypeptides specific to c9FTD/ALS. *Neuron* 77, 639–646.
- Atanasio, A., Decman, V., White, D., Ramos, M., Ikiz, B., Lee, H.C., Siao, C.J., Brydges, S., LaRosa, E., Bai, Y., et al. (2016). *C9orf72* ablation causes immune dysregulation characterized by leukocyte expansion, autoantibody production, and glomerulonephropathy in mice. *Sci. Rep.* 6, 23204.
- Belzil, V.V., Bauer, P.O., Prudencio, M., Gendron, T.F., Stetler, C.T., Yan, I.K., Pregent, L., Daugherty, L., Baker, M.C., Rademakers, R., et al. (2013). Reduced *C9orf72* gene expression in c9FTD/ALS is caused by histone trimethylation, an epigenetic event detectable in blood. *Acta Neuropathol.* 126, 895–905.
- Boeynaems, S., Bogaert, E., Michiels, E., Gijselinck, I., Sieben, A., Jovičić, A., De Baets, G., Scheveneels, W., Steyaert, J., Cuijt, I., et al. (2016). Drosophila screen connects nuclear transport genes to DPR pathology in c9ALS/FTD. *Sci. Rep.* 6, 20877.
- Chew, J., Gendron, T.F., Prudencio, M., Sasaguri, H., Zhang, Y.J., Castaneda-Casey, M., Lee, C.W., Jansen-West, K., Kurti, A., Murray, M.E., et al. (2015). Neurodegeneration. *C9ORF72* repeat expansions in mice cause TDP-43 pathology, neuronal loss, and behavioral deficits. *Science* 348, 1151–1154.
- Ciura, S., Lattante, S., Le Ber, I., Latouche, M., Tostivint, H., Brice, A., and Kabashi, E. (2013). Loss of function of *C9orf72* causes motor deficits in a zebrafish model of amyotrophic lateral sclerosis. *Ann. Neurol.* 74, 180–187.
- Cooper-Knock, J., Walsh, M.J., Higginbottom, A., Robin Highley, J., Dickman, M.J., Edbauer, D., Ince, P.G., Wharton, S.B., Wilson, S.A., Kirby, J., et al. (2014). Sequestration of multiple RNA recognition motif-containing proteins by *C9orf72* repeat expansions. *Brain* 137, 2040–2051.
- DeJesus-Hernandez, M., Mackenzie, I.R., Boeve, B.F., Boxer, A.L., Baker, M., Rutherford, N.J., Nicholson, A.M., Finch, N.A., Flynn, H., Adamson, J., et al. (2011). Expanded GGGGCC hexanucleotide repeat in noncoding region of *C9ORF72* causes chromosome 9p-linked FTD and ALS. *Neuron* 72, 245–256.
- Devlin, A.C., Burr, K., Borooah, S., Foster, J.D., Cleary, E.M., Geti, I., Vallier, L., Shaw, C.E., Chandran, S., and Miles, G.B. (2015). Human iPSC-derived motoneurons harbouring TARDBP or *C9ORF72* ALS mutations are dysfunctional despite maintaining viability. *Nat. Commun.* 6, 5999.
- Donnelly, C.J., Zhang, P.W., Pham, J.T., Haeusler, A.R., Mistry, N.A., Vidensky, S., Daley, E.L., Poth, E.M., Hoover, B., Fines, D.M., et al. (2013). RNA toxicity from the ALS/FTD *C9ORF72* expansion is mitigated by antisense intervention. *Neuron* 80, 415–428.
- Farg, M.A., Sundaramoorthy, V., Sultana, J.M., Yang, S., Atkinson, R.A., Levin, V., Halloran, M.A., Gleeson, P.A., Blair, I.P., Soo, K.Y., et al. (2014). *C9ORF72*, implicated in amyotrophic lateral sclerosis and frontotemporal dementia, regulates endosomal trafficking. *Hum. Mol. Genet.* 23, 3579–3595.
- Freibaum, B.D., Lu, Y., Lopez-Gonzalez, R., Kim, N.C., Almeida, S., Lee, K.H., Badders, N., Valentine, M., Miller, B.L., Wong, P.C., et al. (2015). GGGGCC repeat expansion in *C9orf72* compromises nucleocytoplasmic transport. *Nature* 525, 129–133.
- Gendron, T.F., Bieniek, K.F., Zhang, Y.J., Jansen-West, K., Ash, P.E., Caulfield, T., Daugherty, L., Dunmore, J.H., Castaneda-Casey, M., Chew, J., et al. (2013). Antisense transcripts of the expanded *C9ORF72* hexanucleotide repeat form nuclear RNA foci and undergo repeat-associated non-ATG translation in c9FTD/ALS. *Acta Neuropathol.* 126, 829–844.
- Gendron, T.F., Belzil, V.V., Zhang, Y.J., and Petruccielli, L. (2014). Mechanisms of toxicity in c9FTD/ALS. *Acta Neuropathol.* 127, 359–376.
- Gendron, T.F., van Blitterswijk, M., Bieniek, K.F., Daugherty, L.M., Jiang, J., Rush, B.K., Pedraza, O., Lucas, J.A., Murray, M.E., Desaro, P., et al. (2015). Cerebellar c9RAN proteins associate with clinical and neuropathological characteristics of *C9ORF72* repeat expansion carriers. *Acta Neuropathol.* 130, 559–573.
- Gijselinck, I., Van Langenhove, T., van der Zee, J., Sleegers, K., Philtjens, S., Kleinberger, G., Janssens, J., Bettens, K., Van Cauwenbergh, C., Pereson, S., et al. (2012). A *C9orf72* promoter repeat expansion in a Flanders-Belgian cohort with disorders of the frontotemporal lobar degeneration–amyotrophic lateral sclerosis spectrum: a gene identification study. *Lancet Neurol.* 11, 54–65.
- Gijselinck, I., Van Moesvelde, S., van der Zee, J., Sieben, A., Engelborghs, S., De Bleecker, J., Ivanou, A., Deryck, O., Edbauer, D., Zhang, M., et al. (2015). The *C9orf72* repeat size correlates with onset age of disease, DNA methylation

- and transcriptional downregulation of the promoter. *Mol. Psychiatry.* <http://dx.doi.org/10.1038/mp.2015.159>.
- Harms, M.B., Cady, J., Zaidman, C., Cooper, P., Bali, T., Allred, P., Cruchaga, C., Baughn, M., Libby, R.T., Pestronk, A., et al. (2013). Lack of C9ORF72 coding mutations supports a gain of function for repeat expansions in amyotrophic lateral sclerosis. *Neurobiol. Aging* 34, 2234.e13–2234.e19.
- Heiman, M., Schaefer, A., Gong, S., Peterson, J.D., Day, M., Ramsey, K.E., Suárez-Fariñas, M., Schwarz, C., Stephan, D.A., Surmeier, D.J., et al. (2008). A translational profiling approach for the molecular characterization of CNS cell types. *Cell* 135, 738–748.
- Hukema, R.K., Riemsdijk, F.W., Melhem, S., van der Linde, H.C., Severijnen, L.A., Edbauer, D., Maas, A., Charlet-Berguerand, N., Willemsen, R., and van Swieten, J.C. (2014). A new inducible transgenic mouse model for C9orf72-associated GGGGCC repeat expansion supports a gain-of-function mechanism in C9orf72-associated ALS and FTD. *Acta Neuropathol. Commun.* 2, 166.
- Jovićić, A., Mertens, J., Boeynaems, S., Bogaert, E., Chai, N., Yamada, S.B., Paul, J.W., 3rd, Sun, S., Herdy, J.R., Bieri, G., et al. (2015). Modifiers of C9orf72 dipeptide repeat toxicity connect nucleocytoplasmic transport defects to FTD/ALS. *Nat. Neurosci.* 18, 1226–1229.
- Koppers, M., Blokhuis, A.M., Westeneng, H.J., Terpstra, M.L., Zundel, C.A., Vieira de Sá, R., Schellevis, R.D., Waite, A.J., Blake, D.J., Veldink, J.H., et al. (2015). C9orf72 ablation in mice does not cause motor neuron degeneration or motor deficits. *Ann. Neurol.* 78, 426–438.
- Kordasiewicz, H.B., Staneck, L.M., Wancewicz, E.V., Mazur, C., McAlonis, M.M., Pytel, K.A., Artates, J.W., Weiss, A., Cheng, S.H., Shihabuddin, L.S., et al. (2012). Sustained therapeutic reversal of Huntington's disease by transient repression of huntingtin synthesis. *Neuron* 74, 1031–1044.
- Kwon, I., Xiang, S., Kato, M., Wu, L., Theodoropoulos, P., Wang, T., Kim, J., Yun, J., Xie, Y., and McKnight, S.L. (2014). Poly-dipeptides encoded by the C9orf72 repeats bind nucleoli, impede RNA biogenesis, and kill cells. *Science* 345, 1139–1145.
- Lagier-Tourenne, C., Baughn, M., Rigo, F., Sun, S., Liu, P., Li, H.R., Jiang, J., Watt, A.T., Chun, S., Katz, M., et al. (2013). Targeted degradation of sense and antisense C9orf72 RNA foci as therapy for ALS and frontotemporal degeneration. *Proc. Natl. Acad. Sci. USA* 110, E4530–E4539.
- Lee, Y.B., Chen, H.J., Peres, J.N., Gomez-Deza, J., Attig, J., Stalekar, M., Troakes, C., Nishimura, A.L., Scotter, E.L., Vance, C., et al. (2013). Hexanucleotide repeats in ALS/FTD form length-dependent RNA foci, sequester RNA binding proteins, and are neurotoxic. *Cell Rep.* 5, 1178–1186.
- Levine, T.P., Daniels, R.D., Gatta, A.T., Wong, L.H., and Hayes, M.J. (2013). The product of C9orf72, a gene strongly implicated in neurodegeneration, is structurally related to DENN Rab-GEFs. *Bioinformatics* 29, 499–503.
- Ling, S.C., Polymenidou, M., and Cleveland, D.W. (2013). Converging mechanisms in ALS and FTD: disrupted RNA and protein homeostasis. *Neuron* 79, 416–438.
- Liu, E.Y., Russ, J., Wu, K., Neal, D., Suh, E., McNally, A.G., Irwin, D.J., Van Deerlin, V.M., and Lee, E.B. (2014). C9orf72 hypermethylation protects against repeat expansion-associated pathology in ALS/FTD. *Acta Neuropathol.* 128, 525–541.
- Mackenzie, I.R., Frick, P., and Neumann, M. (2014). The neuropathology associated with repeat expansions in the C9ORF72 gene. *Acta Neuropathol.* 127, 347–357.
- Mackenzie, I.R., Frick, P., Grässer, F.A., Gendron, T.F., Petruccielli, L., Cashman, N.R., Edbauer, D., Kremmer, E., Prudlo, J., Troost, D., and Neumann, M. (2015). Quantitative analysis and clinico-pathological correlations of different dipeptide repeat protein pathologies in C9ORF72 mutation carriers. *Acta Neuropathol.* 130, 845–861.
- May, S., Hornburg, D., Schludi, M.H., Arzberger, T., Rentzsch, K., Schwenk, B.M., Grässer, F.A., Mori, K., Kremmer, E., Banzhaf-Strathmann, J., et al. (2014). C9orf72 FTLD/ALS-associated Gly-Ala dipeptide repeat proteins cause neuronal toxicity and Unc119 sequestration. *Acta Neuropathol.* 128, 485–503.
- McMillan, C.T., Russ, J., Wood, E.M., Irwin, D.J., Grossman, M., McCluskey, L., Elman, L., Van Deerlin, V., and Lee, E.B. (2015). C9orf72 promoter hypermethylation is neuroprotective: neuroimaging and neuropathologic evidence. *Neurology* 84, 1622–1630.
- Miller, T.M., Pestronk, A., David, W., Rothstein, J., Simpson, E., Appel, S.H., Andres, P.L., Mahoney, K., Allred, P., Alexander, K., et al. (2013). An antisense oligonucleotide against SOD1 delivered intrathecally for patients with SOD1 familial amyotrophic lateral sclerosis: a phase 1, randomised, first-in-man study. *Lancet Neurol.* 12, 435–442.
- Mizielinska, S., Lashley, T., Norona, F.E., Clayton, E.L., Ridder, C.E., Fratta, P., and Isaacs, A.M. (2013). C9orf72 frontotemporal lobar degeneration is characterised by frequent neuronal sense and antisense RNA foci. *Acta Neuropathol.* 126, 845–857.
- Mizielinska, S., Grönke, S., Niccoli, T., Ridder, C.E., Clayton, E.L., Devoy, A., Moens, T., Norona, F.E., Woollacott, I.O., Pietrzyk, J., et al. (2014). C9orf72 repeat expansions cause neurodegeneration in *Drosophila* through arginine-rich proteins. *Science* 345, 1192–1194.
- Mori, K., Arzberger, T., Grässer, F.A., Gijsselinck, I., May, S., Rentzsch, K., Weng, S.M., Schludi, M.H., van der Zee, J., Cruts, M., et al. (2013a). Bidirectional transcripts of the expanded C9orf72 hexanucleotide repeat are translated into aggregating dipeptide repeat proteins. *Acta Neuropathol.* 126, 881–893.
- Mori, K., Lammich, S., Mackenzie, I.R., Forné, I., Zilow, S., Kretzschmar, H., Edbauer, D., Janssens, J., Kleinberger, G., Cruts, M., et al. (2013b). hnRNP A3 binds to GGGGCC repeats and is a constituent of p62-positive/TDP43-negative inclusions in the hippocampus of patients with C9orf72 mutations. *Acta Neuropathol.* 125, 413–423.
- Mori, K., Weng, S.M., Arzberger, T., May, S., Rentzsch, K., Kremmer, E., Schmid, B., Kretzschmar, H.A., Cruts, M., Van Broeckhoven, C., et al. (2013c). The C9orf72 GGGGCC repeat is translated into aggregating dipeptide-repeat proteins in FTLD/ALS. *Science* 339, 1335–1338.
- O'Rourke, J.G., Bogdanik, L., Muhammad, A.K.M.G., Gendron, T.F., Kim, K.J., Austin, A., Cady, J., Liu, E.Y., Zarrow, J., Grant, S., et al. (2015). C9orf72 BAC transgenic mice display typical pathologic features of ALS/FTD. *Neuron* 88, 892–901.
- O'Rourke, J.G., Bogdanik, L., Yáñez, A., Lall, D., Wolf, A.J., Muhammad, A.K., Ho, R., Carmona, S., Vit, J.P., Zarrow, J., et al. (2016). C9orf72 is required for proper macrophage and microglial function in mice. *Science* 351, 1324–1329.
- Peters, O.M., Cabrera, G.T., Tran, H., Gendron, T.F., McKeon, J.E., Metterville, J., Weiss, A., Wightman, N., Salameh, J., Kim, J., et al. (2015). Human C9orf72 hexanucleotide expansion reproduces RNA foci and dipeptide repeat proteins but not neurodegeneration in BAC transgenic mice. *Neuron* 88, 902–909.
- Renton, A.E., Majounie, E., Waite, A., Simón-Sánchez, J., Rollinson, S., Gibbs, J.R., Schymick, J.C., Laaksovirta, H., van Swieten, J.C., Myllykangas, L., et al.; ITALSGEN Consortium (2011). A hexanucleotide repeat expansion in C9ORF72 is the cause of chromosome 9p21-linked ALS-FTD. *Neuron* 72, 257–268.
- Rossi, S., Serrano, A., Gerbino, V., Giorgi, A., Di Francesco, L., Nencini, M., Bozzo, F., Schininà, M.E., Bagni, C., Cestra, G., et al. (2015). Nuclear accumulation of mRNAs underlies G4C2-repeat-induced translational repression in a cellular model of C9orf72 ALS. *J. Cell Sci.* 128, 1787–1799.
- Russ, J., Liu, E.Y., Wu, K., Neal, D., Suh, E., Irwin, D.J., McMillan, C.T., Harms, M.B., Cairns, N.J., Wood, E.M., et al. (2015). Hypermethylation of repeat expanded C9orf72 is a clinical and molecular disease modifier. *Acta Neuropathol.* 129, 39–52.
- Sareen, D., O'Rourke, J.G., Meera, P., Muhammad, A.K., Grant, S., Simpkinson, M., Bell, S., Carmona, S., Ornelas, L., Sahabian, A., et al. (2013). Targeting RNA foci in iPSC-derived motor neurons from ALS patients with a C9ORF72 repeat expansion. *Sci. Transl. Med.* 5, 208ra149.
- Schludi, M.H., May, S., Grässer, F.A., Rentzsch, K., Kremmer, E., Küpper, C., Klopstock, T., Arzberger, T., and Edbauer, D.; German Consortium for Frontotemporal Lobar Degeneration; Bavarian Brain Banking Alliance (2015). Distribution of dipeptide repeat proteins in cellular models and C9orf72

- mutation cases suggests link to transcriptional silencing. *Acta Neuropathol.* **130**, 537–555.
- Sharma, S., Rakoczy, S., and Brown-Borg, H. (2010). Assessment of spatial memory in mice. *Life Sci.* **87**, 521–536.
- Smith, R.A., Miller, T.M., Yamanaka, K., Monia, B.P., Condon, T.P., Hung, G., Lobsiger, C.S., Ward, C.M., McAlonis-Downes, M., Wei, H., et al. (2006). Antisense oligonucleotide therapy for neurodegenerative disease. *J. Clin. Invest.* **116**, 2290–2296.
- Su, Z., Zhang, Y., Gendron, T.F., Bauer, P.O., Chew, J., Yang, W.Y., Fostvedt, E., Jansen-West, K., Belzil, V.V., Desaro, P., et al. (2014). Discovery of a biomarker and lead small molecules to target r(GGGGCC)-associated defects in c9FTD/ALS. *Neuron* **83**, 1043–1050.
- Suzuki, N., Maroof, A.M., Merkle, F.T., Koszka, K., Intoh, A., Armstrong, I., Moccia, R., Davis-Dusenberry, B.N., and Eggan, K. (2013). The mouse C9ORF72 ortholog is enriched in neurons known to degenerate in ALS and FTD. *Nat. Neurosci.* **16**, 1725–1727.
- Therrien, M., Rouleau, G.A., Dion, P.A., and Parker, J.A. (2013). Deletion of C9ORF72 results in motor neuron degeneration and stress sensitivity in *C. elegans*. *PLoS ONE* **8**, e83450.
- Tran, H., Almeida, S., Moore, J., Gendron, T.F., Chalasani, U., Lu, Y., Du, X., Nickerson, J.A., Petrucelli, L., Weng, Z., and Gao, F.B. (2015). Differential toxicity of nuclear RNA foci versus dipeptide repeat proteins in a Drosophila model of C9ORF72 FTD/ALS. *Neuron* **87**, 1207–1214.
- van Blitterswijk, M., DeJesus-Hernandez, M., Niemantsverdriet, E., Murray, M.E., Heckman, M.G., Diehl, N.N., Brown, P.H., Baker, M.C., Finch, N.A., Bauer, P.O., et al. (2013). Association between repeat sizes and clinical and pathological characteristics in carriers of C9ORF72 repeat expansions (Xpansize-72): a cross-sectional cohort study. *Lancet Neurol.* **12**, 978–988.
- van Blitterswijk, M., Gendron, T.F., Baker, M.C., DeJesus-Hernandez, M., Finch, N.A., Brown, P.H., Daugherty, L.M., Murray, M.E., Heckman, M.G., Jiang, J., et al. (2015). Novel clinical associations with specific C9ORF72 transcripts in patients with repeat expansions in C9ORF72. *Acta Neuropathol.* **130**, 863–876.
- Wen, X., Tan, W., Westergard, T., Krishnamurthy, K., Markandaiah, S.S., Shi, Y., Lin, S., Schneider, N.A., Monaghan, J., Pandey, U.B., et al. (2014). Antisense proline-arginine RAN dipeptides linked to C9ORF72-ALS/FTD form toxic nuclear aggregates that initiate in vitro and in vivo neuronal death. *Neuron* **84**, 1213–1225.
- Wheeler, T.M., Leger, A.J., Pandey, S.K., MacLeod, A.R., Nakamori, M., Cheng, S.H., Wentworth, B.M., Bennett, C.F., and Thornton, C.A. (2012). Targeting nuclear RNA for in vivo correction of myotonic dystrophy. *Nature* **488**, 111–115.
- Wojciechowska, M., and Krzyzosiak, W.J. (2011). Cellular toxicity of expanded RNA repeats: focus on RNA foci. *Hum. Mol. Genet.* **20**, 3811–3821.
- Xi, Z., Zinman, L., Moreno, D., Schymick, J., Liang, Y., Sato, C., Zheng, Y., Ghani, M., Dib, S., Keith, J., et al. (2013). Hypermethylation of the CpG island near the G4C2 repeat in ALS with a C9orf72 expansion. *Am. J. Hum. Genet.* **92**, 981–989.
- Xi, Z., Zhang, M., Bruni, A.C., Maletta, R.G., Colao, R., Fratta, P., Polke, J.M., Sweeney, M.G., Mudanohwo, E., Nacmias, B., et al. (2015). The C9orf72 repeat expansion itself is methylated in ALS and FTLD patients. *Acta Neuropathol.* **129**, 715–727.
- Xu, Z., Poidevin, M., Li, X., Li, Y., Shu, L., Nelson, D.L., Li, H., Hales, C.M., Gearing, M., Wingo, T.S., and Jin, P. (2013). Expanded GGGGCC repeat RNA associated with amyotrophic lateral sclerosis and frontotemporal dementia causes neurodegeneration. *Proc. Natl. Acad. Sci. USA* **110**, 7778–7783.
- Yang, D., Abdallah, A., Li, Z., Lu, Y., Almeida, S., and Gao, F.B. (2015). FTD/ALS-associated poly(GR) protein impairs the Notch pathway and is recruited by poly(GA) into cytoplasmic inclusions. *Acta Neuropathol.* **130**, 525–535.
- Zhang, D., Iyer, L.M., He, F., and Aravind, L. (2012). Discovery of novel DENN proteins: implications for the evolution of eukaryotic intracellular membrane structures and human disease. *Front. Genet.* **3**, 283.
- Zhang, Y.J., Jansen-West, K., Xu, Y.F., Gendron, T.F., Bieniek, K.F., Lin, W.L., Sasaguri, H., Caulfield, T., Hubbard, J., Daugherty, L., et al. (2014). Aggregation-prone c9FTD/ALS poly(GA) RAN-translated proteins cause neurotoxicity by inducing ER stress. *Acta Neuropathol.* **128**, 505–524.
- Zhang, K., Donnelly, C.J., Haeusler, A.R., Grima, J.C., Machamer, J.B., Steinwald, P., Daley, E.L., Miller, S.J., Cunningham, K.M., Vidensky, S., et al. (2015). The C9orf72 repeat expansion disrupts nucleocytoplasmic transport. *Nature* **525**, 56–61.
- Zhang, Y.J., Gendron, T.F., Grima, J.C., Sasaguri, H., Jansen-West, K., Xu, Y.F., Katzman, R.B., Gass, J., Murray, M.E., Shinohara, M., et al. (2016). C9ORF72 poly(GA) aggregates sequester and impair HR23 and nucleocytoplasmic transport proteins. *Nat. Neurosci.* Published online March 21, 2016. <http://dx.doi.org/10.1038/nn.4272>.
- Zu, T., Gibbons, B., Doty, N.S., Gomes-Pereira, M., Huguet, A., Stone, M.D., Margolis, J., Peterson, M., Markowski, T.W., Ingram, M.A., et al. (2011). Non-ATG-initiated translation directed by microsatellite expansions. *Proc. Natl. Acad. Sci. USA* **108**, 260–265.
- Zu, T., Liu, Y., Bañez-Coronel, M., Reid, T., Pleznikova, O., Lewis, J., Miller, T.M., Harms, M.B., Falchook, A.E., Subramony, S.H., et al. (2013). RAN proteins and RNA foci from antisense transcripts in C9ORF72 ALS and frontotemporal dementia. *Proc. Natl. Acad. Sci. USA* **110**, E4968–E4977.